Titre: Title:	Study of thermal and mechanical properties of styrene-methyl methacrylate copolymers
Auteur: Author:	Fang He
Date:	1989
Type:	Mémoire ou thèse / Dissertation or Thesis
Référence: Citation:	He, F. (1989). Study of thermal and mechanical properties of styrene-methyl methacrylate copolymers [Master's thesis, École Polytechnique de Montréal]. PolyPublie. https://publications.polymtl.ca/56718/

UNIVERSITE DE MONTREAL

STUDY OF THERMAL AND MECHANICAL PROPERTIES OF STYRENE-METHYL METHACRYLATE COPOLYMERS

par

Fang He

DEPARTEMENT DE GENIE CHIMIQUE

ECOLE POLYTECHNIQUE

MEMOIRE PRESENTE EN VUE DE L'OBTENTION

DU GRADE DE MAITRE ES SCIENCES APPLIQUEES (M.Sc.A.)

Janvier 1989

ISBN 0-315-52726-9

Canada

UNIVERSITE DE MONTREAL

ECOLE POLYTECHNIQUE

Ce mémoire intitulé:

STUDY OF THERMAL AND MECHANICAL PROPERTIES OF STYRENE-METHYL METHACRYLATE COPOLYMERS

présenté par: Fang He

en vue de l'obtention du grade de: M.Sc.A.

a été dûment accepté par le jury d'examen constitué de:

M. Henry P. Schreiber, Ph.D., président

M. Pierre Bataille, Ph.D.

M. Slawomir Sapieha, Ph.D.

SOMMAIRE

Le styrène (S) et le méthacrylate de méthyle (MAM) sont deux monomères qui ont atteint un degré de consommation tel qu'ils sont considérés maintenant comme des commodités.

La copolymérisation de ces deux monomères pour obtenir un polymère statistique ou en bloc est effectuée d'une façon courante dans l'industrie. Le procédé pour obtenir une copolymérisation alternée est cependant beaucoup plus complexe. Il nécessite l'utilisation d'un solvant et il génère une quantité importante d'homopolymères comme sous-produit. Cette complexité a découragé beaucoup de chercheurs et d'industriels à utiliser ces copolymères dans leurs travaux.

En 1983, des chercheurs ont développé une méthode simple pour fabriquer le copolymère alterné de S et de MAM.

Le but de ce projet est de polymériser ces deux monomères selon la méthode indiquée par ces chercheurs, d'étudier les propriétés thermiques et mécaniques du polymère alterné et de les comparer avec d'autres copo-

lymères de S-MAM (statistiques et en bloc), afin de relier les propriétés du polymère avec sa composition et sa structure chimique.

Tel qu'indiqué, le copolymère alterné de styrène et de méthacrylate de méthyle a été polymérisé dans notre laboratoire. Les autres polymères utilisés dans cette étude: polystyrène (PS), polyméthacrylate de méthyle (PMAM) ainsi que les copolymères statistiques et en bloc de S-MAM, ont été obtenus de divers manufacturiers.

Tous ces échantillons ont été caractérisés pour leurs masses moléculaires par chromatographie sur gel (GPC) ainsi que pour leurs compositions par résonance magnétique nucléaire (RMN).

L'énergie d'activation (Ea) pour la dégradation du polystyrène et des copolymères a été évaluée par la méthode d'isothermes ainsi que par la méthode de comparaison multi-expérimentale. A cet effet, une thermobalance a été utilisée. La méthode de comparaison multi-expérimentale s'est avérée comme étant la meilleure méthode pour mesurer l'énergie d'activation de dégradation thermique.

La stabilité des homopolymères (PS et PMAM), des

copolymères de S-MAM et des mélanges des PS et PMAM a été mesurée et comparée par la technique de thermogravimétrie (TG). La stabilité du copolymère alterné de S-MAM est plus basse que prévue. On attribue ceci à la présence de résidu de l'agent complexant utilisé pour la copolymérisation. La comparaison des stabilités entre les copolymères et des mélanges de PS-PMAM avec les prédictions mathématiques montre que le polystyrène a un effet stabilisant au début de la dégradation dans le système de PS-PMAM.

Les propriétés mécaniques de tous les échantillons ont été testées à l'aide de la machine à traction. Le copolymère en bloc a des propriétés de tension plus élevées que le copolymère alterné et le copolymère statistique de S-MAM.

Les températures des transitions vitreuses de ces polymères ont été étudiées par le calorimètre différentielle (DSC). En tenant compte de leurs masses moléculaires, l'ordre des transitions vitreuses est le suivant: copolymère alterné > copolymère en bloc > copolymère statistique. Le copolymère alterné a la température de transition vitreuse la plus élevée.

Le mélange des polymères est une méthode rapide et

économique pour obtenir des nouveaux matériaux, elle est utilisée très souvent par les scientifiques et les ingénieurs. PS et PMAM sont deux polymères incompatibles. Pour les polymères incompatibles, plusieurs méthode peuvent être envisagées pour bien disperser un polymère dans l'autre. Nous pouvons citer, par exemple, les méthodes suivantes: introduction de groupes interactifs, réticulation, modification mineure de la structure, introduction de compatibilisateurs, etc.. L'introduction d'un compatibilisateur est le moyen le plus simple de toutes les méthodes possibles. Un compatibilisateur est un composant qui aide à diminuer la tension interfaciale dans le mélange. Souvent, c'est un copolymère en bloc ou greffé qui a des segments identiques ou miscibles avec les deux polymères du mélange. Par ce principe, la possibilité pour S-MAM copolymère d'être compatibilisateur dans le mélange de PS et PMAM a été évaluée par clarté optique, test mécanique dynamique et DSC. Le test mécanique dynamique a montré que le copolymère en bloc de S-MAM a un effet de compatibilisant pour le mélange de polystyrène et polyméthacrylate de méthyle. Le copolymère alterné n'a cependant pas cet effet.

ABSTRACT

Polystyrene (PS) and polymethyl methacrylate (PMMA) are two widely used polymers and may be considered as commodity polymers. Block, random and alternating copolymers of these two monomers are also produced industrially. The usual method for making the alternating copolymer is an expensive one, and the copolymer obtained contains a large amount of polystyrene homopolymer. In 1983, researchers have developed a simpler method to polymerize the S-MMA alternating copolymers, thus it became easier to obtain this copolymer. The objective of this project is to polymerize the S-MMA alternating copolymer, study its thermal and mechanical properties, compare these properties with those of the other kinds of S-MMA copolymers (block and random copolymers), and relate the properties of the polymer with its chemical structure.

The activation energy of thermal degradation of polystyrene and four S-MMA copolymers were determined by isothermal method and multi-experimental comparison method (multiple heating rates method). The multi-experimental comparison method has been considered the most reliable method for measuring the activation energy of polymer's thermal degradation.

The thermal stabilities of the copolymers and PS-PMMA blends were measured and compared by thermogravimetry. The comparison of the degradation of the copolymers and blends with homopolymers (PS and PMMA) showed that polystyrene has a stabilizing effect in PS-PMMA system.

The mechanical properties of the copolymers were tested. The S-MMA block copolymers has higher tensile properties than S-MMA alternating and random copolymers.

The glass transition temperatures of the four copolymers were measured with differential scanning calorimetry (DSC), the order was found to be: alternating copolymer > block copolymer > random copolymer.

Since polymer blending becomes a technique more and more used for developing new materials, the compatibility of polystyrene (PS) with polymethyl methacrylate (PMMA) as well as the effect of S-MMA copolymer in PS-PMMA system were examined by optical clarity, dynamic mechanical test and DSC. The dynamic mechanical test showed that the S-MMA block copolymer has a compatibilizing effect for PS-PMMA blend.

ACKNOWLEDGEMENTS

I would like to express my gratitude to Professor P. Bataille for his guidance, assistance and financial support.

I would like to thank Mr. A. Lachapelle for carrying out the GPC experiments, Mr. A. Désilets for his kind assistance in thermobalance operation, and Mme. S. Bilodeau for performing the NMR test.

Also, I would like to thank the technicians of Chemical Engineering Department in Ecole Polytechnique of Montreal and my colleagues for their encouragement and suggestions during my study.

CONTENTS

List of Tables

LIST of FIGURES

LIST of SYMBOLS

A	:	frequency factor
E	:	tensile modulus (Young's modulus)
Ea	:	Arrhenius energy of activation
E^*	:	complex modulus
E'	:	dynamic tensile storage modulus
E"	:	dynamic tensile loss modulus
n	:	reaction order
N	:	Avogadro's number
R	:	gas constant
T	:	absolute temperature
T_f	:	extrapolated onset temperature in thermogram of DSC
Tg	:	glass transition temperature
Tg^{∞}	:	the Tg at infinite molecular weight
w_o	:	initial weight of reactant
w_f	:	final weight of the sample after the reaction is completed
w_t	:	weight of reactant at time t
x_A	:	the fraction of polymer A in weight, volume or moles
α	:	conversion of thermal degradation
β	:	heating rate (°C/min)

δ : the phase angle

$\tan\delta$: the dissipation factor (loss factor, damping)

ϵ : strain

ϵ_y : yield strain

σ : stress

σ_y : yield stress

ω : the angular frequency

Chapter I

INTRODUCTION

Modern life is unthinkable without polymers. Evidence of our dependence on them is all around us, such as elastomer, plastic, fiber, paint, adhesive, etc.. Polymerization is the most important way to get polymeric materials to satisfy our various requirement. In a homopolymerization reaction, the addition of the monomer to the polymer growing chain may lead to different structures of the polymer following the way the monomer addition is made. For instance, the monomer addition may be a head to tail type or a head to head type, see Fig. 1.

For copolymerization, it is even more complex, not only the way the monomer addition might vary but also the sequence of addition of the monomers. Many types of copolymers may thus be obtained. If a sequence of A "mer" is followed by a sequence of B "mer", it is called block copolymer (poly(A-b-B)); if a B "mer" sequence is grafted on a A "mer" backbone, is called graft copolymer (poly(A-g-B)); there is also random copolymer (poly(A-co-B) where in the copolymer chain appears at random either as A "mer" or a B

Fig. 1 Head to tail and head to head polystyrenes.

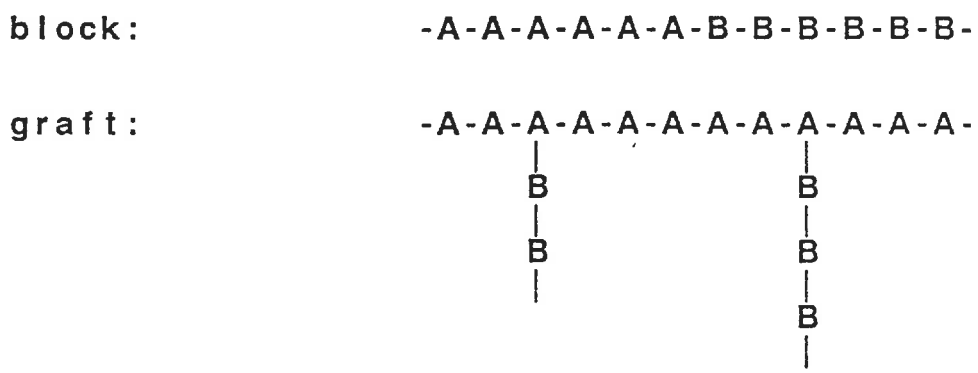

Fig. 2 Different types of copolymers

"mer"; the fourth type of copolymer is the alternating copolymer (poly(A-alt-B)) where A "mer" and B "mer" appear in the copolymer chain alternately. See Fig. 2.

Styrene (S) and methyl methacrylate (MMA) being two well known and readily available monomers, various copolymers were polymerized using these two monomers. In fact, the block and random copolymers of styrene and methyl methacrylate have already been produced industrially[1]. The alternating copolymerization of S and MMA has also been done, but the procedure is cumbersome as the copolymerization is performed in organic medium. And it usually leads to an expensive product containing high level of homopolymer[2]. Besides, the properties of this alternating copolymer is very poorly studied. According to the literature research, only its thermal degradation in air has been studied by Hurduc and co-workers[3]. In 1983, Bataille and co-workers[4,5] found the method of using simple laboratory equipment to polymerize S-MMA alternating copolymer (poly(S-alt-MMA)) in aqueous phase with zinc chloride as complexing agent. Then, it became easier to get large amount of poly(S-alt-MMA). The objective of my project is to polymerize and purify poly(S-alt-MMA), study its thermal properties (degradation, stability, stabilization, glass transition temperature) and mechanical properties; and to compare with those of other available S-MMA copolymers

(block and random), in order to relate the properties of a copolymer with its chemical structure.

Physical blending of polymers is a more rapid and less expensive route to meeting the demands of the market-place than the development of new polymers. The physical properties of multi-component polymeric materials and subsequently their utility is crucially determined by their compatibility. Practically, most of polymers are incompatible[6-8]. Several methods have been developed to enhance compatibility, such as introduction of interacting groups, cross-linking, interpenetrating network formation, minor modification of structure, use of compatibilizer, etc.. Among these, using compatibilizer is the simplest way. Compatibilizer is a substance which can lower the interfacial tension and consequently help to achieve a fine dispersion phases. Often a A-B block or graft copolymer is taken to be the compatibilizer for polymer A-polymer B blend (details in section II. 5 and IV. 6).

Polystyrene (PS)-polymethyl methacrylate (PMMA) blend have been proved to be an incompatible system (see section IV. 6). Therefore, the possibility for S-MMA copolymers to be compatibilizers for PS-PMMA blend was tested as part of this project.

Chapter II

THEORETICAL PRINCIPLES

In this chapter, the theoretical principles of main techniques used in this project are discussed.

II. 1 THERMAL ANALYSIS

Thermal analysis is the measurement of a property of a material as a function of temperature. In this study, two of the major thermal analysis techniques were employed —— thermogravimetry (TG) and differential scanning calorimetry (DSC).

II.1.A Thermogravimetry

Thermogravimetry is the measurement of the change in weight of a substance as the temperature of its environment

is varied in a controlled manner. It is often used to study thermal stability of polymeric materials in polymer science. It has also been intensively and successfully used to investigate kinetic parameters of polymer thermal degradation.

The simplified expression for the reaction undergone by polymers during thermal degradation is:

$$aA \longrightarrow bB + cC$$

where a, b, c: numbers of molecules.

A: original solid reactant;

B: solid residue. For the reaction where all the product are volatile, b = 0;

C: gaseous product evolved;

The rate of reaction may be expressed as[9]:

$$d\alpha/dt = \beta d\alpha/dT = f(\alpha)k(T)g(\alpha,T)h(\sum_i X_i Y_i \ldots) \qquad (1)$$

where t = reaction time;

β = heating rate, °C/min;

α = conversion defined as

$$\alpha = (w_o - w_t)/(w_o - w_f)$$

w_o = initial weight of reactant;

w_t = weight of reactant at time t;

w_f = final weight of the sample after the reaction is completed;

T = absolute temperature.

In Equ. 1, $f(\alpha)$ is the function of conversion α, k(T) is the function of temperature, $g(\alpha,T)$ contains conversion -temperature cross-terms, and $h(\Sigma X_i Y_i \ldots)$ contains all other variables which affect the reaction rate, such as pressure, gaseous flow rate, gaseous composition, physical and geometric properties of the sample and cross-terms with themselves.

In general treatments of polymer degradation in a thermobalance, it is assumed that all the variables of $h(\Sigma X_i Y_i \ldots)$ are either maintained constant or do not affect the reaction rate, i.e., $h(\Sigma X_i Y_i \ldots) = 1$. It is assumed also that no conversion-temperature cross-term exist, $g(\alpha,T) = 1$. Thus

$$d\alpha/dt = \beta d\alpha/dT = f(\alpha)k(T) \qquad (2)$$

here, k(T) is often modeled successfully by the Arrhenius equation even in the case where the degradation mechanism is complex:

$$k(T) = A \exp(-Ea/RT) \qquad (3)$$

where A = frequency factor;

Ea = Arrhenius energy of activation;

R = gas constant;

Substituting Equ. 3 into Equ. 2,

$$d\alpha/dt = \beta\ d\alpha/dT = A\ f(\alpha)\ \exp(-Ea/RT) \qquad (4)$$

Since Equ. 4 is a very much simplified form of Equ. 1, all the influence of function $g(\alpha, T)$ and $h(\Sigma X_i\ Y_i \ldots)$ are lumped into $f(\alpha)$ term in Equ. 4, it is impossible to model $f(\alpha)$ for many systems by an unit equation like the function k(T). The most simple and frequently used expression for $f(\alpha)$ is[9]:

$$f(\alpha) = (1-\alpha)^n \qquad (5)$$

then

$$d\alpha/dt = \beta\ d\alpha/dT = A[\exp(-Ea/RT)](1-\alpha)^n \qquad (6)$$

In the case where $w_f = 0$, i.e., no solid residue, it is written more conveniently as

$$f(w_t) = -w_t{}^n \qquad (7)$$

$$dw_t/dt = \beta\, dw_t/dT = -A[\exp(-Ea/RT)]w_t^{\,n} \qquad (8)$$

where n, in analogy to homogeneous chemical kinetics, is called the order of reaction. These expressions of $f(\alpha)$ are more successful in isothermal experiments than in non-isothermal ones where the changes of temperature further complicates the situation.

Equations 6 and 8 have been extended in various ways in order to relate the kinetic parameters with values that can be determined experimentally. Below is the discussion of some methods most often used.

II.1.A.1 Freeman and Carroll's differential method[10]

Starting from Equ. 8, since in our case, $w_f=0$ (the more general equation — Equ. 6 can be derived in exactly the same way), the natural logarithmic form of Equ. 8 is

$$\ln(-dw_t/dt) = \ln(A) - Ea/RT + n*\ln(w_t) \qquad (9)$$

Equ. 9 can be written for two different temperatures, as

$$\ln(-dw_t/dt)_1 = \ln(A) - E_a/RT_1 + n*\ln(w_{t\,1}) \qquad (10)$$

$$\ln(-dw_t/dt)_2 = \ln(A) - E_a/RT_2 + n*\ln(w_{t\,2}) \qquad (11)$$

and Equ. 11 is subtracted from Equ. 10

$$\ln(-dw_t/dt)_1 - \ln(-dw_t/dt)_2 = (-E_a/R)*(1/T_1 - 1/T_2) + n*[\ln(w_{t1}) - \ln(w_{t2})]$$

$$\Delta\ln(-dw_t/dt) = -(E_a/R)*\Delta(1/T) + n*\Delta\ln(w_t)$$

$$[\Delta\ln(-dw_t/dt)]/\Delta(1/T) = -(E_a/R) + n*[\Delta\ln(w_t)]/\Delta(1/T) \qquad (12)$$

According to Equation 12, in an experiment where the heating rate is constant, if $\Delta[\ln(-dw_t/dt)]/\Delta(1/T)$ is plotted against $[\Delta\ln(w_t)]/\Delta(1/T)$, activation energy E_a and reaction order n will be obtained from the intercept and the slope.

Since this method needs only one non-isothermal experiment to determine the kinetic parameters in a large temperature range, and it can be obtained if these parameters change while the temperature is varied, It has become the most popular method for non-isothermal data.

II.1.A.2 Simple differential method

Dividing Equation 8 by $-W_t^n$ gives

$$(-dw_t/dt)/w_t^n = A \exp(-E_a/RT) \quad (13)$$

$$\ln[(-dw_t/dt)/w_t^n] = \ln A - Ea/RT \quad (14)$$

Basing on equation 14, the reaction order n is determined by substituting various values of n into the equation until the curve of $\ln(-dw_t/dt)/w_t^n$ versus 1/T fits a straight line. Then the activation energy E_a is calculated from the slope[11].

These two methods have the same disadvantage: the reliability of Equ. 5 or Equ. 7 is smaller in non-isothermal experiment than in isothermal one.

II.1.A.3 Isothermal method

Equation 8 can be used directly to solve A, E_a and n from three sets of data points for $-dw_t/dt$, T and w_t on the TG curve. A more accurate way is to carry out the experiment in an isothermal condition, and plot $\ln(-dw_t/dt)$ versus

$\ln(w_t)$, then the reaction order n can be obtained from the slope (Equ. 9). The activation energy can be evaluated by two isothermal TG experiments[12], from the two intercepts of $\ln(-dw_t/dt)$ versus $\ln(w_t)$ curves.

As mentioned above, Equations 5 and 7 are better approximations in isothermal experiments than in non-isothermal experiments. Therefore, this method was used in this work.

II.1.A.4 Multi-experimental comparison method

Those three method described previously are based on Equations 6 and 8, but these two equations do not apply to all the polymers' degradation processes[9]. In order to avoid modelling of $f(\alpha)$, a multi-experimental comparison method has been developed:

Integrate Equ. 4 as follows:

$$d\alpha/dT = (A/\beta)\, f(\alpha)\, \exp(-Ea/RT) \qquad (4)$$

$$d\alpha/f(\alpha) = (A/\beta)\, \exp(-Ea/RT)\, dT \qquad (15)$$

$$F(\alpha) = \int_0^{\alpha} \frac{d\alpha}{f(\alpha)} = \int_{T_0}^{T} (A/\beta)[\exp(-Ea/RT)]\, dT$$

$$= \frac{AEa}{\beta R}\left(\frac{e^{-x}}{x} - \int_x^{\infty}\frac{e^{-x}}{x}\,dx\right)$$

$$- \frac{AEa}{\beta R}\left(\frac{e^{-x_o}}{x_o} - \int_{x_o}^{\infty}\frac{e^{-x}}{x}\,dx\right) \qquad (16)$$

$$x = Ea/RT$$

$$x_o = Ea/RT_o$$

It is assumed that the lower limit T_o is low enough that the integral at To is negligible for usual polymer degradation cases, then,

$$F(\alpha) = \frac{AEa}{\beta R}\left(\frac{e^{-x}}{x} - \int_x^{\infty}\frac{e^{-x}}{x}\,dx\right)$$

$$= \frac{AEa}{\beta R}\,p\left(\frac{Ea}{RT}\right) \qquad (17)$$

Logarithmic form of Equ. 17 is

$$\log F(\alpha) = \log(AEa/R) - \log(\beta) + \log p(Ea/RT) \qquad (18)$$

Doyle[13] has found that for $Ea/RT \geq 20$,

$$\log p(Ea/RT) \approx -2.315 - 0.457Ea/RT \qquad (19)$$

Substituting Equ. 19 into Equ. 18, one obtains

$$\log F(\alpha) \approx \log(AEa/R) - \log \beta - 2.315 - 0.457Ea/RT$$
$$\approx \text{constant} - \log \beta - 0.457Ea/RT \qquad (20)$$

Appendix I[14,15] lists log p(Ea/RT) values for various Ea/RT. According to Equ. 20, If experiments are performed at several heating rates, one fixes the conversion, and plot log β against 1/T, the slope will be approximately 0.457Ea/R. Once $Ea_{approx.}$ is obtained, $Ea/RT_{approx.}$ may be calculated, this $Ea/RT_{approx.}$ can be used to reevaluate the constant, "0.457" in Equ. 20, using the data in Appendix I, then a more approached Ea, $Ea_{corrected}$, will be calculated by the help of the reevaluated constant. Of course this iterative process can be repeated until the result does not change anymore, but it has been demonstrated that a single iteration is sufficient, see Appendix IV and Ref. 16.

The most important advantage of this method is that it is independent on the form of $f(\alpha)$. Also in this method, if the mechanism of degradation changes with temperature or conversion, the curve of log β versus 1/T will bend or the lines at different conversion will not be parallel. Another advantage of this method is that only

two kinds of value need to be read from TG curves: conversions and temperatures. Comparing with the methods described previously, in multi-experimental comparison method, less points have to be read from the thermogram and these values are read more accurately.

More precisely, this method is called the "multi-experimental integral comparison method". There is also a "multi-experimental differential comparison method", based also on the same equation, Equ. 4. It has been demonstrated that the integral method is more precise and simple than the differential method[16]. The integral method has been considered to be the absolute method in determining the thermal activation energy of polymer degradation[16].

Up to here, methods those are most frequently used for investigating apparent activation energy of polymer thermal degradation have been discussed, although it did not cover the whole spectrum of the various possible methods.

II.1.B Differential Scanning Calorimetry (DSC)

Differential Scanning Calorimetry (DSC) is developed from differential thermal analysis (DTA) technique.

It is well known that if the temperature of a polymer sample is raised, the sample may run into the following phenomena: glass transition, crystallization, melting, cross-linking, oxidation and degradation. These physical and chemical changes are accompanied by thermal effects. Differential scanning calorimeter (DSC) is designed to measure sample's thermal capacity as a function of temperature, i.e., to measure the thermal effects of a sample while it is heated or cooled in a programmed manner.

Fig. 3 and Fig. 4 are the center part and the block diagram of DSC.

The reference material is a substance thermally inert in the temperature region of measurement except for slight and gradual changes in heat capacity with temperature.

During an experiment, the temperature of the sample and of the reference is varied linearly with time. While the temperature is varying, if a physical or chemical change takes place, the heat absorbed or evolved by the sample is compensated by adding or subtracting an equivalent amount of electrical energy to a heater located in the sample holder. The continuous and automatic adjustment of heater power (energy per unit time) necessary to keep the sample holder temperature identical to that of the reference holder provides an electrical signal equivalent to the thermal behavior of the sample. By recording the variable

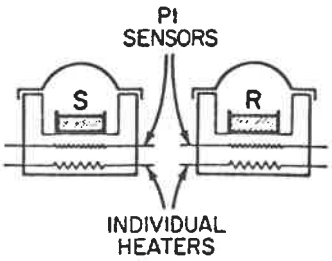

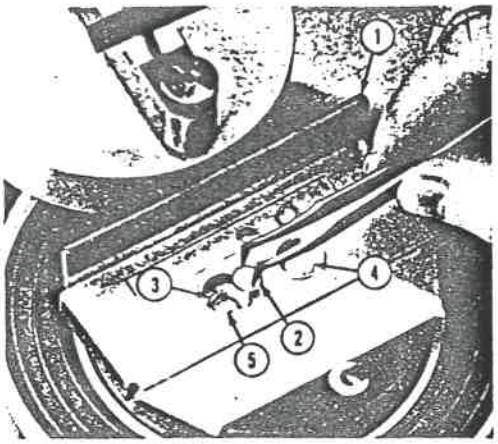

1 *Sample Handling Tray*
2 *Sample Holder Cover (with holes)*
3 *Sample Holder for Samples*
4 *Sample Holder for Reference Materials*
5 *Sample Pan*

Model DSC-2 Sampling Provisions

Fig. 3 Center part of DSC.

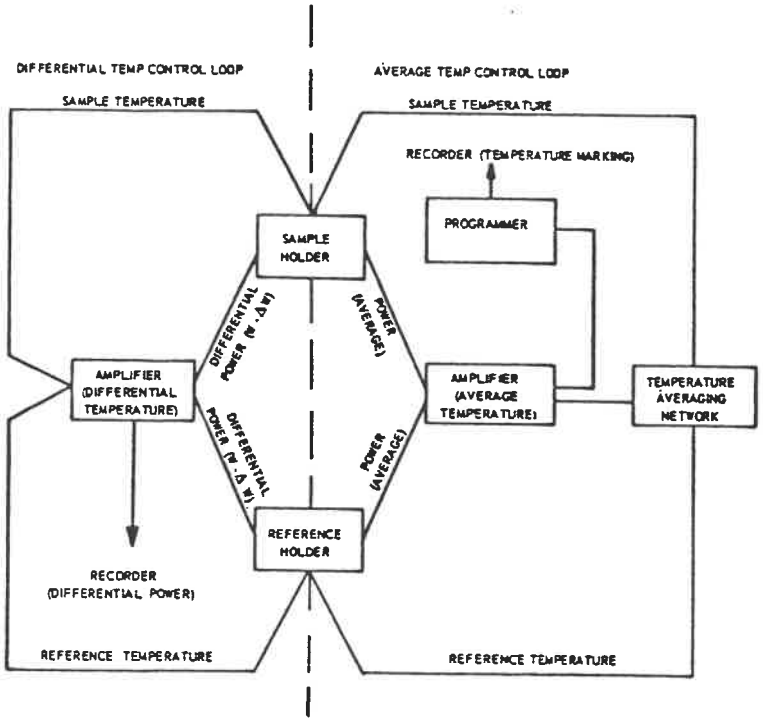

Fig. 4 Block diagram of the Perkin-Elmer DSC

part of the electrical signal or the differential power, a record of the thermal behavior of the sample as function of temperature is obtained.

Fig. 5 is a generalized DSC thermogram of a polymer.

II. 2 POLYMER STABILIZATION

The following simplified kinetic scheme for hydrocarbon oxidation has been suggested[17]:

Initiation:

$$RH \longrightarrow R\bullet \qquad (21)$$

$$R\bullet + O_2 \longrightarrow ROO\bullet \qquad (22)$$

Propagation:

$$ROO\bullet + RH \longrightarrow ROOH + R\bullet \qquad (23)$$

$$ROOH \longrightarrow RO\bullet + HO\bullet \qquad (24)$$

$$ROOH + RH \longrightarrow RO\bullet + R\bullet + H_2O \qquad (25)$$

$$RO\bullet + RH \longrightarrow ROH + R\bullet \qquad (26)$$

$$HO\bullet + RH \longrightarrow H_2O + R\bullet \qquad (27)$$

Termination:

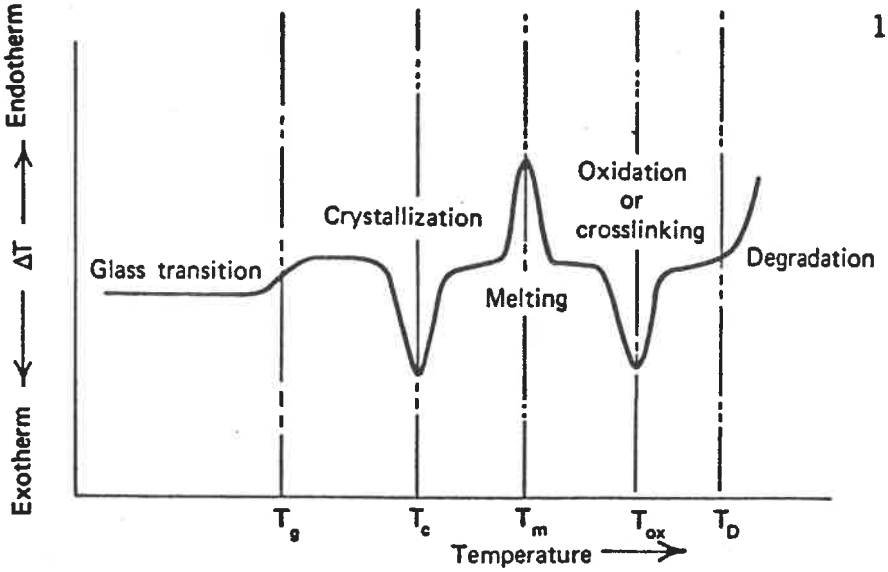

Fig. 5 A generalized DSC thermogram of a polymer.

(1) $A\cdot + ROO\cdot \longrightarrow R{-}O{-}O{-}A$

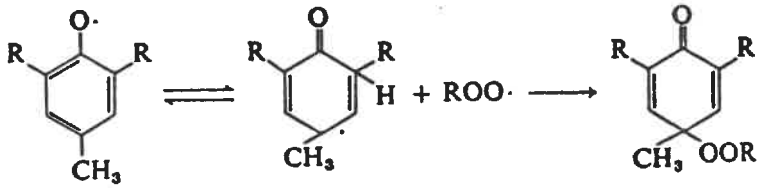

(2) $A\cdot + ROO\cdot \longrightarrow ROOH + A'$

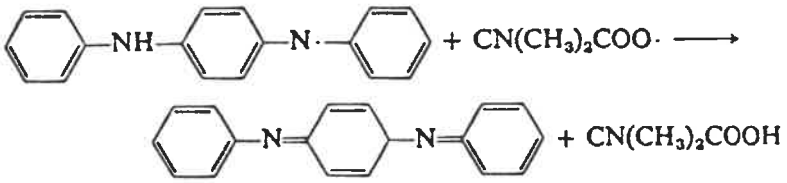

(3) $A\cdot + A\cdot \longrightarrow A{-}A$

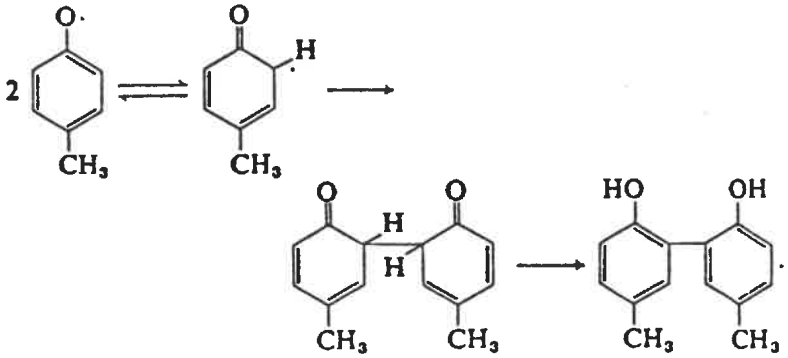

(4) $A\cdot + A\cdot \longrightarrow HA + A'$

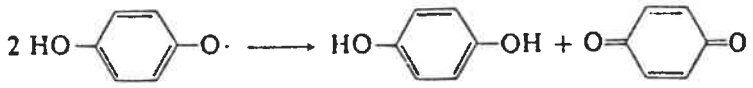

Fig. 6[18] Stabilisation by Chain Termination: $ROO\cdot + HA \rightarrow ROOH + A\cdot$. Reactions of $A\cdot$.

$$2R\bullet \longrightarrow R\text{-}R \qquad (28)$$

$$ROO\bullet + R\bullet \longrightarrow ROOR \qquad (29)$$

$$2ROO\bullet \longrightarrow \text{non-radical products} + O_2 \qquad (30)$$

It is evident that stabilization can be effected at several stages in this mechanism. Stabilizers such as hindered phenol and aryl amine terminate the propagating chain by donating hydrogen or electron:

$$ROO\bullet + AH \longrightarrow ROOH + A\bullet \qquad (31)$$

where AH is the stabilizer. The A• radical is stabilized by virtue of their multiple resonance structures so that it does not continue to propagate the oxidative reaction. They may also undergo a sequence of secondary reactions such as following:

$$ROO\bullet + A\bullet \longrightarrow ROOA \qquad (32)$$

$$ROO\bullet + A\bullet \longrightarrow ROOH + A' \qquad (33)$$

$$A\bullet + A\bullet \longrightarrow A\text{-}A \qquad (34)$$

$$A\bullet + A\bullet \longrightarrow AH + A' \qquad (35)$$

See Fig. 6[18].

These chain termination stabilizers are called primary antioxidant.

Sulfur and phosphorous compounds stabilize polymers by decomposing peroxide as follows:

$$RSSR + R'OOH \longrightarrow RSOSR + R'OH \qquad (36)$$

$$ROOH \xrightarrow{RSOSR \longrightarrow SO_2} \text{inert product} \qquad (37)$$

This kind of stabilizer is called secondary antioxidant. Comparing with primary antioxidant which act only at propagation step, secondary antioxidant decomposes peroxide so that prevent oxidation from the very beginning[17] (Fig. 7). Combination of primary and secondary antioxidant may exhibit a synergistic effect[17] (Fig. 8). Several theories have been proposed to account for these synergism. The explanation most generally accepted is that each component of the stabilizer system function in a way which conserves the other component: decomposition of peroxide into normal product increases the effective concentration of the chain terminator since there are fewer oxidative chains to be interrupted; as the oxidative chains are shortened so that the concentration of peroxide is reduced, then the peroxide decomposer is present at a higher concentration relative to the peroxide formed.

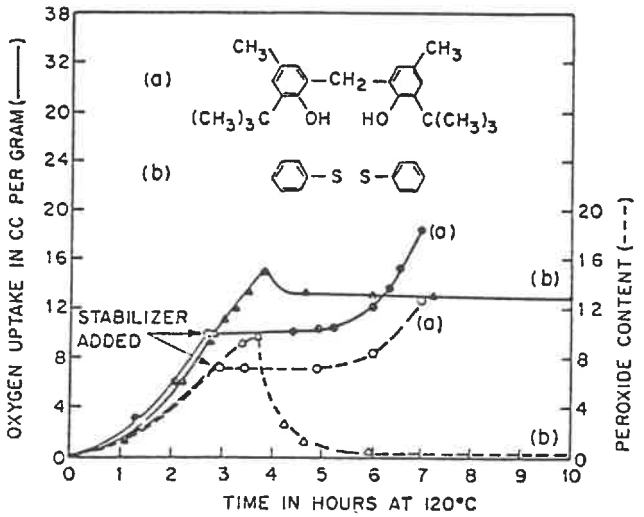

FIG.7[17] Relationship between oxidation rate and peroxide concentration in the oxidation of cumene following addition of (a) 2,2′-methylenebis-(4-methyl-6-*t*-butylphenol) and (b) phenyl disulfide.

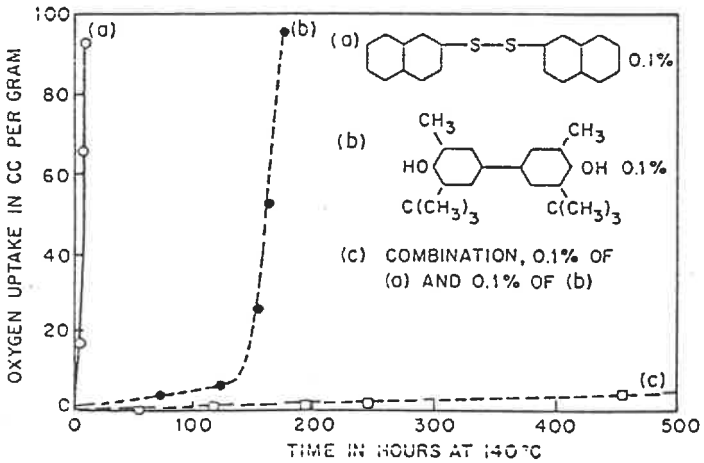

FIG.8[17] Synergism between (a) 2,2′-naphthyl disulfide and (b) 4,4′-bis(2-methyl-6-*t*-butylphenol).

II. 3 STRESS-STRAIN TENSILE PROPERTIES of POLYMERS

Stress-strain test in tension is one of the most informative mechanical experiments for any material[19]. It is done by elongating a sample at a constant rate, the force used to pull the sample, i.e., the stress developed in the sample while it is being stretched, is measured and recorded continuously.

The elongation rates are generally 0.5, 5, 50, and 500 mm/min.

Fig. 9 is the generalized stress-strain tensile curve for plastics. Young's modulus (elastic modulus) is the slope of the initial part of the curve. Fig. 10 shows typical features of several types of polymers.

In Fig. 9, point A is called yield point. For most of ductile materials, during its elongation, when the strain reaches yield strain ϵ_y, necking of the cross section happens. After point A, the stress diminishes. This phenomena is called yielding. The elongation of the neck part after yielding is called cold-drawing. The stress at yield point is named yield stress (σ_y). Here, the stress is apparent stress, i.e., the cross section is supposed to be unchanged. In fact, when a sample is elongated, especially

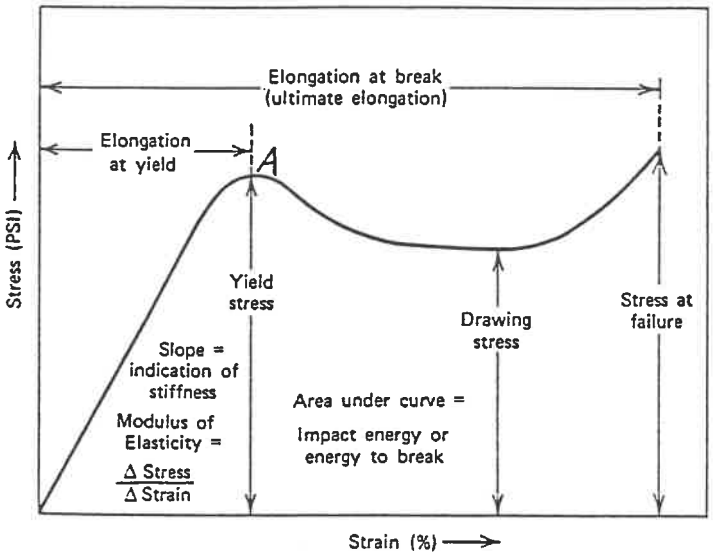

Fig. 9 Generalized tensile stress-strain curve for plastics.

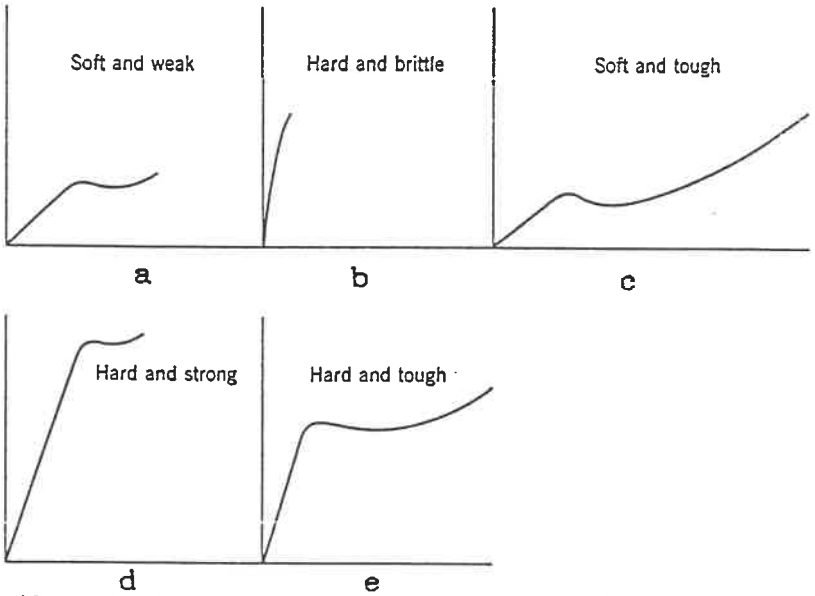

Fig. 10 Tensile stress-strain curves showing features typical of several types of polymers (*Textbook*, Fig. 4-11, from Winding 1961).

when necking occurs, its cross section becomes smaller. True stress is the force applied on sample divided by the true minimum section area. Therefore, the true stress is bigger than the apparent stress. Equations have been deduced to calculate the true stress, and theories have been proposed to explain yielding and cold drawing. Our samples are hard and brittle (their stress-strain curves are of Fig. 10-b type).

Young's modulus can also be measured by compression test [20,21], flexural test[22], and creep test[23]. But the modulus obtained by compression is bigger than the one obtained by tension, see Fig. 11, as defect and microcrack of material act more in tension test than in compression test. The modulus measured by flexure is higher too, because plastic materials do not obey perfectly the classical linear theory of mechanics upon which the modulus calculation equation is based[23]. The creep test is good for long time scale (weeks, months) experiment.

Other methods to measure Young's modulus are vibration[23] and wave propagation techniques[24-26]. In our experiments, only the tensile test was carried out.

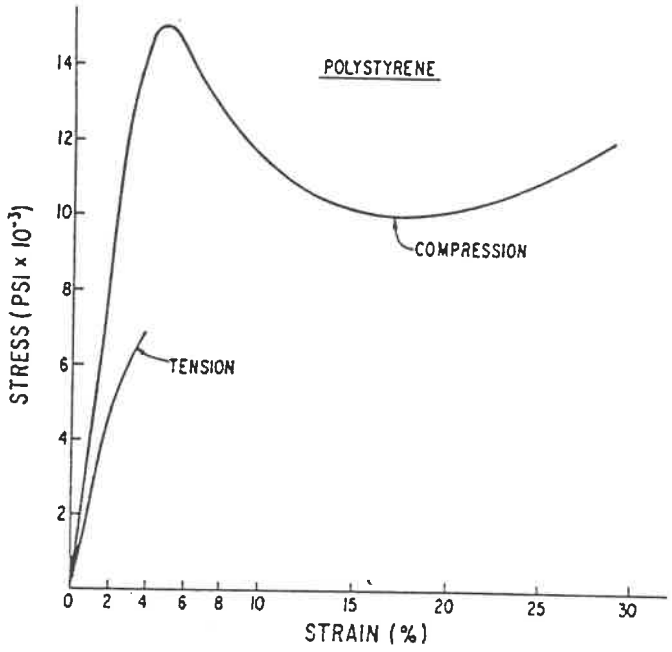

Fig. 11

The stress-strain behavior of a normally brittle polymer such as polystyrene under tension and compression.

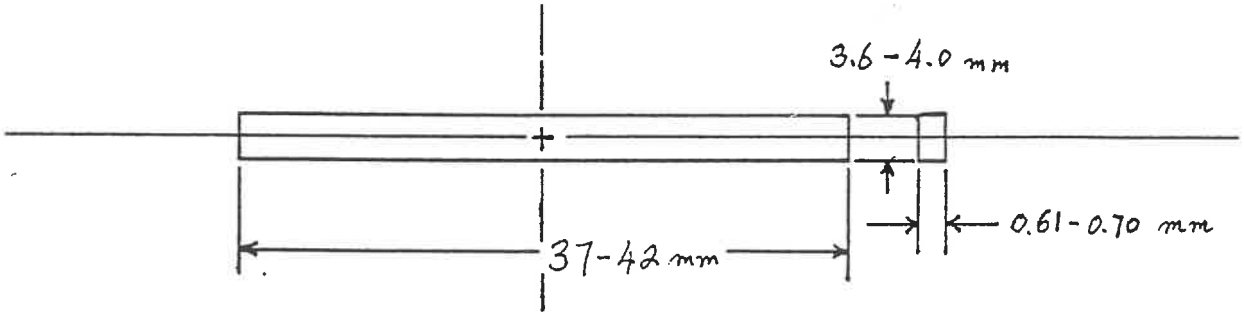

Fig. 12 Sample shape in dynamic mechanical test.

II. 4 DYNAMIC MECHANICAL PROPERTIES of POLYMERS

The unique characteristic of polymers is viscoelasticity, it means that in extreme cases, a polymeric material can behave either as an elastic solid or as a viscous fluid. Therefore, when a strain is applied to such a material, part of the energy is stored elastically and part is lost as heat in the deformation process.

Consider a sample, shaped as shown in Fig. 12, of a polymeric material, if a sinusoidal strain of a certain frequency is applied on one end of the sample, the response stress of the sample measured at another end will vary sinusoidally too, with the same frequency as that of the applied strain, but out of phase, as shown in Fig. 13. The strain ϵ and stress σ can be expressed as

$$\epsilon = \epsilon_o \sin(\omega t) \tag{38}$$

$$\sigma = \sigma_o \sin(\omega t+\delta) \tag{39}$$

where ω = the angular frequency;

δ = the phase angle.

Expanding Equation 39 leads to

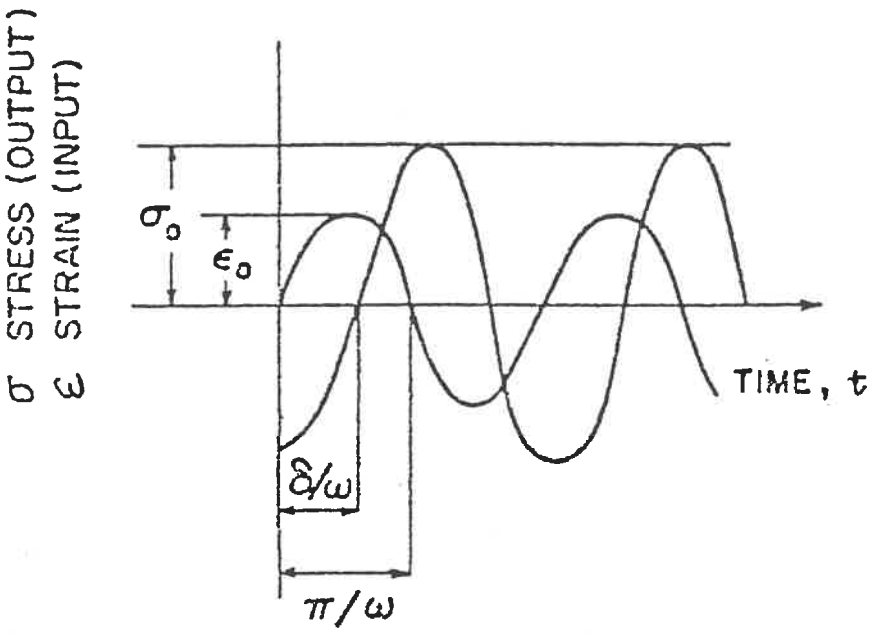

Fig. 13 A sinusoidal stimulus (strain ϵ) and its response (stress σ).

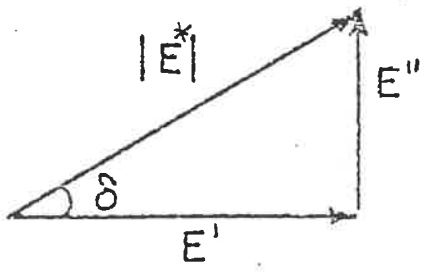

Fig. 14 Relation between $|E^*|$, E' and E".

$$\sigma = \sigma_0 \sin(\omega t)\cos\delta + \sigma_0 \cos(\omega t)\sin\delta \qquad (40)$$

The stress can be considered to consist of two components, one is $\sigma_0 \cos\delta$ which is in phase with the strain, related to the stored elastic energy; another is $\sigma_0 \sin\delta$ which is 90° out of phase with the strain, related to the viscous loss energy. The ratio of the two: $\tan\delta$, is the dissipation factor (or loss factor, damping), an indicator of the relative importance of the elastic aspect as compared to the viscous aspect of the material's behavior. For this reason, Equation 40 is written in the form of

$$\sigma = \epsilon_0 E' \sin\omega t + \epsilon_0 E'' \cos\omega t \qquad (41)$$

$$E' = (\sigma_0/\epsilon_0)\cos\delta \qquad (42)$$

$$E'' = (\sigma_0/\epsilon_0)\sin\delta \qquad (43)$$

$$E''/E' = \tan\delta \qquad (44)$$

E' is the real part of the modulus, called dynamic tensile storage modulus; and E'' is the imaginary part of the modulus, called dynamic tensile loss modulus.

The complex representation for the modulus can be expressed as follows:

$$\epsilon^* = \epsilon_0 \exp(i\omega t) \qquad (45)$$

$$\sigma^* = \sigma_0 \exp i(\omega t+\delta) \qquad (46)$$

$$\sigma^*/\epsilon^* = E^* = (\sigma_o/\epsilon_o)e^{i\delta}$$
$$= (\sigma_o/\epsilon_o)(\cos\delta + i\sin\delta)$$
$$= E' + iE'' \qquad (47)$$

$$|E^*| = (E'^2 + E''^2)^{1/2} = \sigma_o/\epsilon_o \qquad (48)$$

See Fig. 14.

The complex modulus E^* is a function describing completely a material's dynamic mechanical behavior for the case of small strain.

The damping $\tan\delta$ is of special interest to us, as it is extremely sensitive to all kinds of transitions. It can serve as an indicator of homogeneity of a multi-components system. These will be demonstrated in section II.5.B.

II. 5 COMPATIBILITY

Polymer blends are known as physical mixture of two or more polymers. Since copolymers are often expensive, polymer blending is a economic and easy way to achieve new and useful properties.

The properties of the blend is determined primarily by the miscibility of the two polymers. When we say two polymers are miscible, it means that they are thermodynamically mutually soluble, the properties of the blend are nearly the same as those of a random copolymer of the same composition, having one glass transition temperature and so on (See Section II. 5). This case is very rare. If the polymers are immiscible, high interfacial tension and poor adhesion exist at the interface, lead to phase separation. Since most polymer pairs are immiscible, in engineering sense, the term "compatible" is employed for the blend which is homogeneous to the eye and with enhanced physical properties. Compatible does not mean miscible. Two immiscible polymers could be compatible. On the other hand, miscible polymers are compatible.

In the case where two polymers are not compatible, many routes can be taken to get a refined mixture (see Chapter I). The most simple manner is to add a third component which serves as a "compatibilizer". Ideally, this component should be a copolymer constituted of segments that are chemically identical or miscible to those of the respective phases[27-37]. This compatibilizing agent locates at the interface of the two phases, see Fig. 15, its effect is as those of surfactants in water-oil systems, facilitating the mixing of the two immiscible polymers.

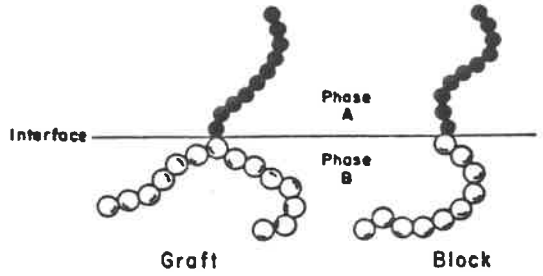

Fig. 15 Ideal location of block-and-graft copolymers at the interface between polymer phases A and B.

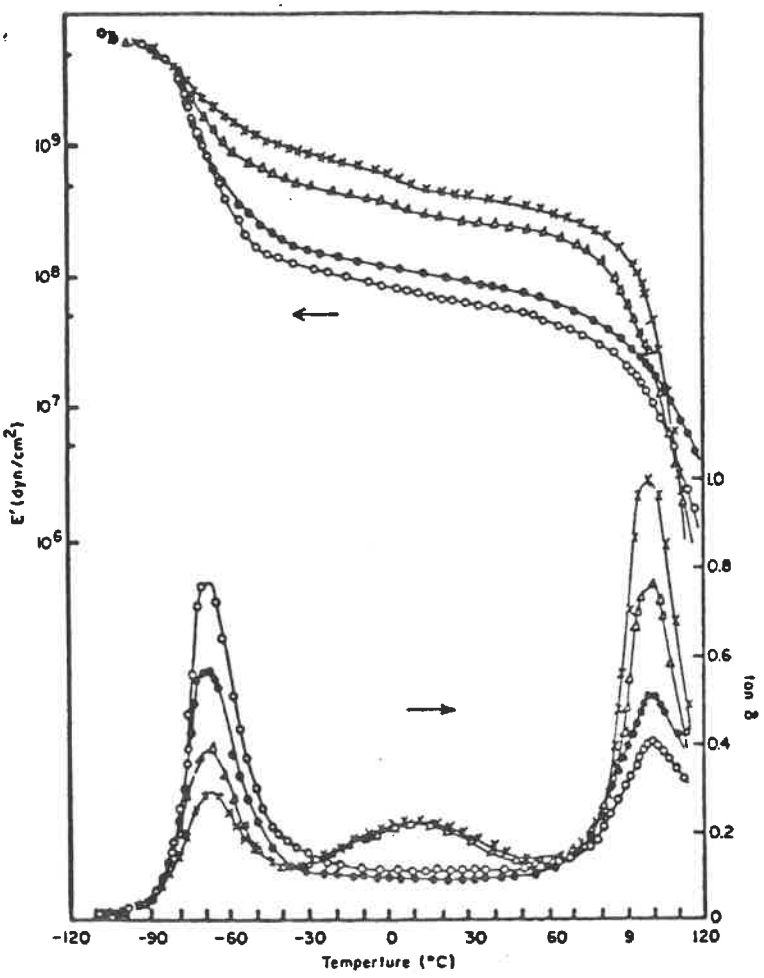

Fig. 39

Fig. 16 Dynamic mechanical properties of a 30% styrene (MW = 15100 for each block) styrene-butadiene-styrene block polymer cast from different solvents which change the relative amounts of continuous and dispersed phases. X = methyl ethyl ketone, △ = ethyl acetate, ● = toluene, O = carbon tetrachloride. [Reprinted from Miyamoto, Kodama, and Shibayama, J. Polymer Sci., A2, 8, 2095 (1970).]

Although it does not change the immiscible state of these two, it does help to "solubilize" one polymer into another, permits a finer dispersion, reduces the interfacial energy between the phases and improves interfacial adhesion. Following are criteria of compatibility.

II.5.A Optical Clarity

Optical clarity is a very convenient indicator of miscibility. A transparent blend signifies either the polymers in the blend are miscible or the dimensions of phases are small compared with optical wavelengths. A cloudy or opaque blend film tells the phase separation or bad mixing.

II.5.B Dynamic mechanical properties and DSC

For a two phases mixture, the dynamic storage modulus versus temperature curve has two steep drops, each one corresponds to one phase's glass transition temperature, as shown in Figure 16. Consequently, the dissipation factor tanδ versus temperature curve has two peaks too. If significant molecular mixing takes place, the transition will

be broadened and their temperatures will shift closer to each other. In the case of complete miscible system, the E'-T curve has only one steep drop, as a random copolymer.

These changes in Tg can also be detected by DSC.

II.5.C Mechanical properties

Tensile test is another way to inform the compatibility of two polymers.

For two compatible polymers, the Young's modulus (E), yield strength (σ_y), ultimate strength (σ_u) and ultimate elongation (ϵ_u) of the blend of these two polymers should follow the additive rule, i.e., the property of the blend can be calculated as:

$$Q_{blend} = xQ_A + (1-x)Q_B \qquad (49)$$

where Q is the property discussed, x is the fraction of polymer A in weight, volume or mole, and the subscripts refer to polymer A and polymer B respectively[27,28,38].

If the two polymers are semi-compatible, where the polymers disperse into each other to a certain degree, the curve of Q_{blend} versus composition will be S-shaped, and in the case of incompatible, U-shaped[38]. But the compatibility

of the blend has not always the same affect on different mechanical properties. For example, in Fig. 17[38], for polymethyl methacrylate-polyurethane blend, the curve of yield strength versus composition indicates that the two polymers are compatible, while semi-compatible according to the modulus and ultimate elongation curves, and incompatible in the case of ultimate strength.

II.5.D Other methods

Other methods to investigate polymer-polymer compatibility are sonic[39-42] and ultrasonic[43-45] velocity measurements in solids or solutions of blends, heat of mixing determination[46], scanning electron microscopy, viscometric study[47-49], and thermal degradation of polymer blend[50,51].

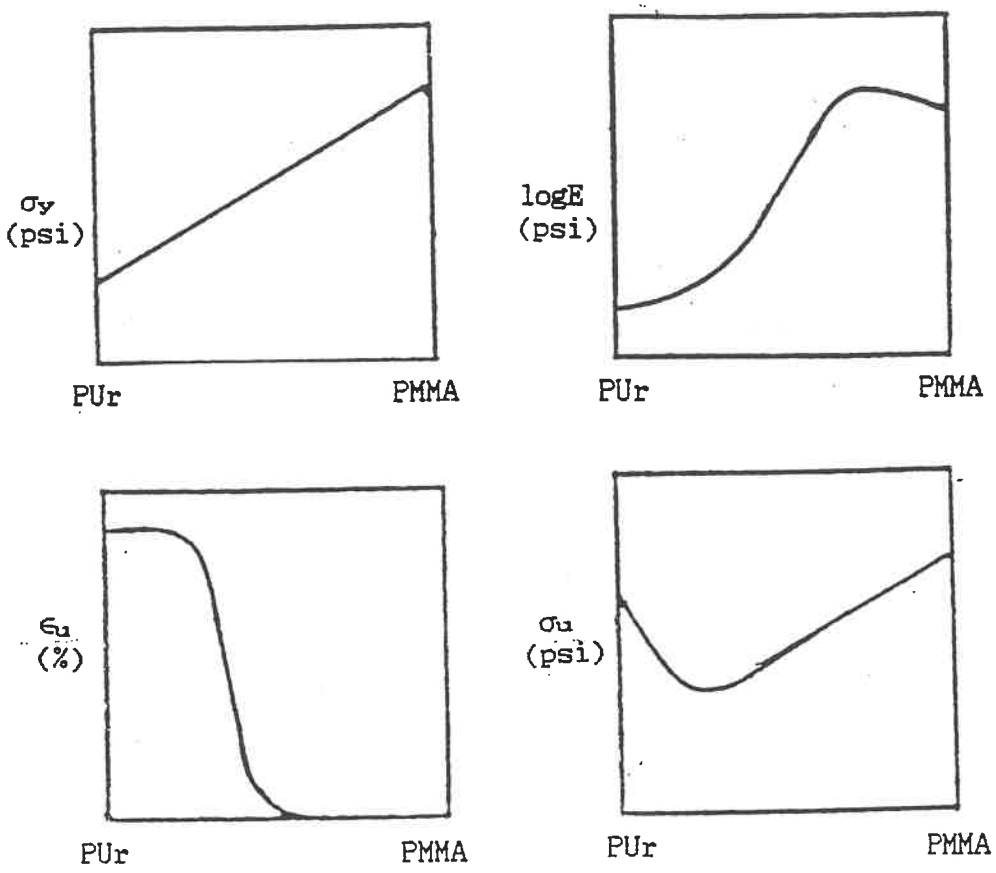

Fig. 17[38] Stress-strain tensile properties (yield strength (σ_y), tensile modulus (E), ultimate strain (ϵ_u) and ultimate strength (σ_u)) of polyurethane-polymethyl methacrylate blend .

Chapter III

MATERIALS AND EXPERIMENTAL PROCEDURE

III. 1 MATERIALS

Styrene-methyl methacrylate alternating copolymer (poly(S-alt-MMA)) was polymerized in our laboratory by emulsion polymerization[4,5] and purified by selective precipitation using toluene as the solvent and ether as the non-solvent[52]. The complete description of its polymerization as well as its characterization is given in Appendix II.

Polystyrene, code 204-00, was supplied by Polysar Ltd., and polymethyl methacrylate, grade VM 100, code 3-1581, was supplied by Rohm and Haas Canada Inc.. P-210-D, P-205-UV-A and NAS are methyl methacrylate-styrene copolymers, they were provided by Richardson Co..

All the polymers were characterized by gel permeation chromatography (GPC) (Model 150-C ALC/GPC, Millipore Waters), employing tetrahydrofuran as solvent, the polymer concentration was 0.05%. The three copolymers supplied by Richardson Co. were further analyzed by nuclear magnetic

resonance (NMR) in order to determine their respective composition and the monomer arrangement on the copolymer chains. The NMR utilized is a Bruker WH-400 spectrometer, recorded at 21°C, C_6D_6 as solvent, 400.13 MHz for ^1H, performed at University of montreal. The results are presented in Table 1.

Table 1

Characterization of Polymers

Sample	Styrene%	$\bar{M}_n$	$\bar{M}_w$	Polydispersity	Polymer type
PS	100	$9.1*10^4$	$1.9*10^5$	2.0	homo-
PMMA	0	$2.7*10^4$	$4.6*10^4$	1.7	homo-
poly(S-alt-MMA)	50	$2.9*10^5$	$1.4*10^6$	4.7	alternating
P-210-D	38.4	$5.4*10^4$	$8.9*10^4$	1.6	block
P-205-UV-A	38.7	$9.1*10^4$	$1.5*10^5$	1.7	block
NAS	69.1	$8.7*10^4$	$1.4*10^5$	1.7	random

Thermal stabilizers Irganox 1010 and Irganox MD-1024 are from Ciba Geigy Corp..

III. 2 THERMAL ANALYSIS

III.2.A Thermogravimetry

In this study, the thermogravimetry was done with a Mettler Thermoanalyzer, type T-E. Its diagram is shown in Fig 18. In the experiment, the thermobalance was started two hours before experiment to attain equilibrium. Aluminium oxide powder, under the trade mark of AnalaR, from BDH Chemical Ltd., was chosen as reference. The balance had been evacuated before the experiment starts. The flow rate of atmosphere gas was 200 ml/min, pressure 1atm. The heating rate was 10°C/min. In every experiment, when the temperature rises to 200°C, it was kept at that temperature for 10 to 25 min in order to remove possibly residual monomer or water in the polymer sample. The time of the isotherm period depended on the sample, it lasted until the TG curve reached a steady line. After isotherm, the temperature was raised to the programmed one in the case of isothermal experiment or increased continuously until all the sample was volatilized in the case of non-isothermal experiment.

Stabilizers were mixed with the powdered polymer.

The samples were in a form of fine powder in order to

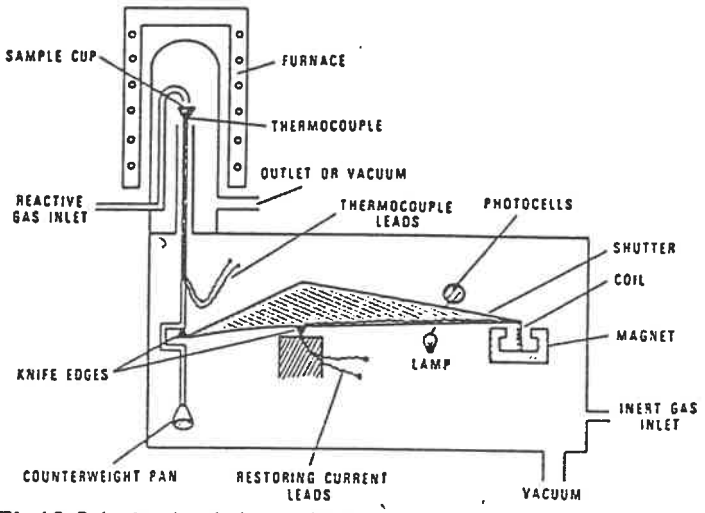

Fig.18 Substitution balance (Mettler thermoanalyzer).

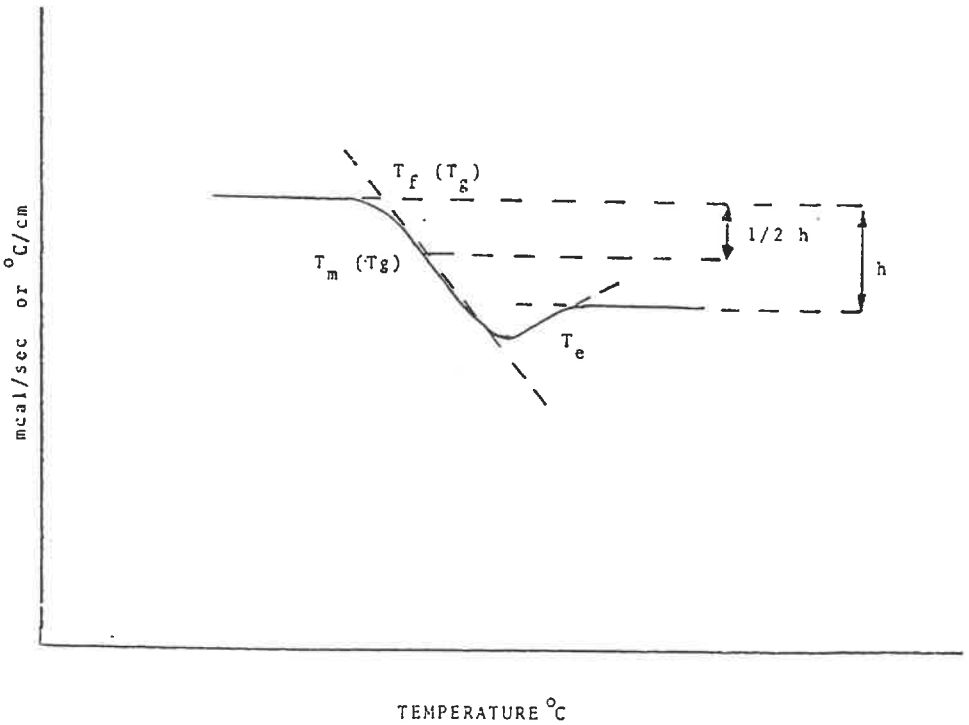

FIG.19 Glass Transition of PMMA (Poly(Methyl Methacrylate)).

overcome diffusion problems of the evolving gases. The average weight of samples was 16 mg.

III.2.B Differential Scanning Calorimetry

A Perkin-Elmer Model DSC-2 calorimeter was used in the experiment. The principle on which the calorimeter works has been explained in section II.1.B.

The experiment was done in nitrogen atmosphere (30 psi), the heating rate was 10°C/min.

In order to erase the thermal histories, every sample was conditioned before measurement by heating it to 160-170°C at the rate of 10°C/min (This temperature is 60 to 70°C higher than their respective T_g's (90 to 105°C) and 100°C lower than their decomposition temperature (more than 260°C)), then cooling it down at 10°C/min to 40°C.

The ASTM D3418 method was employed to determine T_g and T_f, see Fig. 19.

III. 3 BLENDING and COMPRESSION MOLDING

A Plasti-corder Torque Rheometer of C. W. Brabender Instruments Inc. was used to make polymer blends, with 30g head. Brabender is a very commonly used equipment in research laboratory, it can operate with small amount of sample to simulate the action of a Banbury mill, an extruder, or a simple sigma-blade mixer. Comparing with casting from solution, blending with Brabender needs no solvents, hence, it does not need long time and vacuum to dry the blend. The disadvantage of this method is the risk of degradation while mixing at high temperature and high shear rate.

A Wabash Hydraulic Press (Wabash, Indiana) was used to prepare sample sheets by compression molding. The temperature of the two plates of this press can be controlled easily.

In the operation, first, the Brabender head was heated to 220°C. Then, total weight of 25g two or three kinds of polymers in desired proportion were filled into it. The speed was 40 rotations per minute. The blending time lasted until a equilibrium torque was attained.

The hydraulic press was heated to 190°C, the blend

from the Brabender was then put on it, the pressure was kept at 0 ton for 1 minute, then at 2 tons for 30 seconds, to gave enough time for remained gases to escape from the sample. After this, the pressure was increased to 8 tons, and maintained at this level for 10 seconds, the sheets was then taken out and quenched in cold water immediately.

For comparing, another polymer mixture, powder mixture, was prepared by mixing two kinds of polymer powder together. The comparison of Tg's of powder mixture and fusion blend was made in Section IV.6.C.

III. 4 STRESS-STRAIN TENSILE TEST

The tensile properties were measured with Tensile Tester Model 4201 of Instron Corporation at 25°C. The jaw separation rate was 0.5mm/min. Such a slow speed was chosen because the samples are very brittle, and the ultimate elongations are small, about 0.7mm.

The samples were cut from the sheets prepared by compression molding, dimensions are shown in Fig. 20. Since the sheets are hard and brittle, they had to be heated before cutting. The two plates of the manual press were

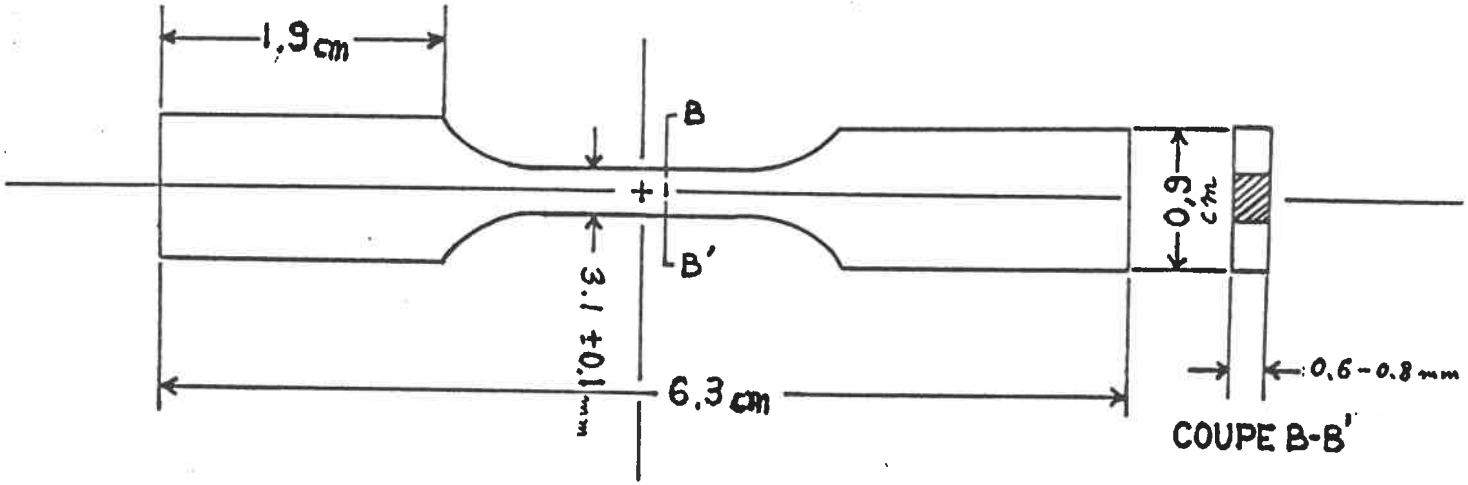

Fig. 20 Dimensions of sample for stress-strain tensile test.

thus heated to 100°C, a sheet was put between the two plates for about 3 minutes, when it became soft, a sample was punched out. Then the sheet was put back on the plate again for about 10 seconds, then another sample was cut. As 100°C is quite low than the samples' decomposition temperature (260°C), degradation was not observed after reheating, i.e., the color of the polymers was not changed.

III. 5 DYNAMIC MECHANIC TEST

The Rheovibron is designed to measure the temperature dependence of the complex modulus E^*, dynamic storage modulus E', dynamic loss modulus E" and dissipation factor tanδ at specific selected frequency.

During measurement, a sinusoidal tensile strain of a fixed frequency (3.5, 11, 35 or 110 Hz for Rheovibron Model DDV-II) is applied to one end of a sample, and the response stress is measured at the other end by a transducer, the phase angle δ between strain and stress in the sample is assessed in a direct-reading method.

Moduli calculation equations are as follows:

$$|E^*| = (2/AD)(L/S)10^9 \quad \text{dyne/cm}^2 \tag{50}$$

$$E' = |E^*|\cos\delta \tag{51}$$

$$E'' = |E^*|\sin\delta \tag{52}$$

where A = instrument constant obtained from the value of the amplitude factor dial when measuring $\tan\delta$.

D = the value of dynamic force dial when valuing $\tan\delta$.

L = sample length (cm);

S = sample's cross section area (cm^2);

Rheovibron Model DDV-II was utilized in this project. The temperature range was about 50 to 120°C. The low limit was set at a temperature well below the sample's Tg, and the up limit was restricted by the $\tan\delta$ range (0-1.7) and the dynamic force range (0 to 1000). The heating rate was controlled by a transformer at 1°C/min.

All the samples were cut from sheets prepared by compression under the same condition, thus, they have the same thermal history.

Chapter IV

RESULTS AND DISCUSSION

IV. 1 ACTIVATION ENERGIES of THERMAL DEGRADATION of POLYSTYRENE and S-MMA COPOLYMERS

The activation energies and reaction orders of thermal degradations of poly(S-alt-MMA) and polystyrene in air and in helium atmospheres were investigated by isothermal method with a thermobalance, the calculation procedure is attached as Appendix III, the results are listed in Table 2. These values were obtained from the plots of $\ln(-dw_t/dt)$ versus $\ln(w_t)$ for these polymers using Equ. 9. The plots are shown in Figures 21-24.

The values of polystyrene obtained here compare well with the results of other workers. For polystyrene in air, Hurduc and co-workers[3] obtained an energy of activation of 184.1 kJ/mole, whereas Wilson and Hamaker[53], Anderson and Freeman[54] both groups working in vacuum attained the activation energy of 255 kJ/mole, Madorsky[55] evaluated a value somewhat lower, of about 230 kJ/mole. Finally, also worked with polystyrene but in an argon atmosphere, Zaitsev got

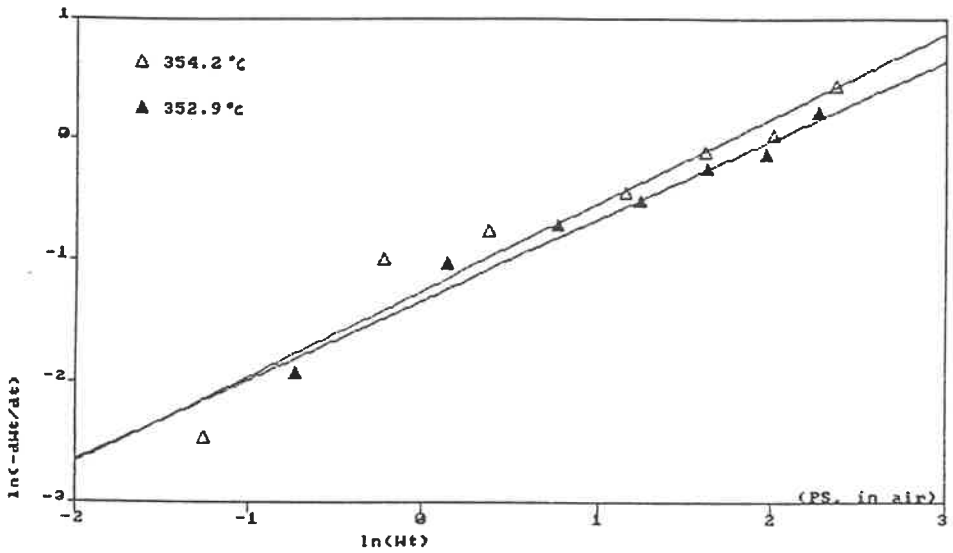

Fig. 21 $\ln(-dw_t/dt)$ versus $\ln(w_t)$ plots for PS isothermal degradation in air atmosphere.

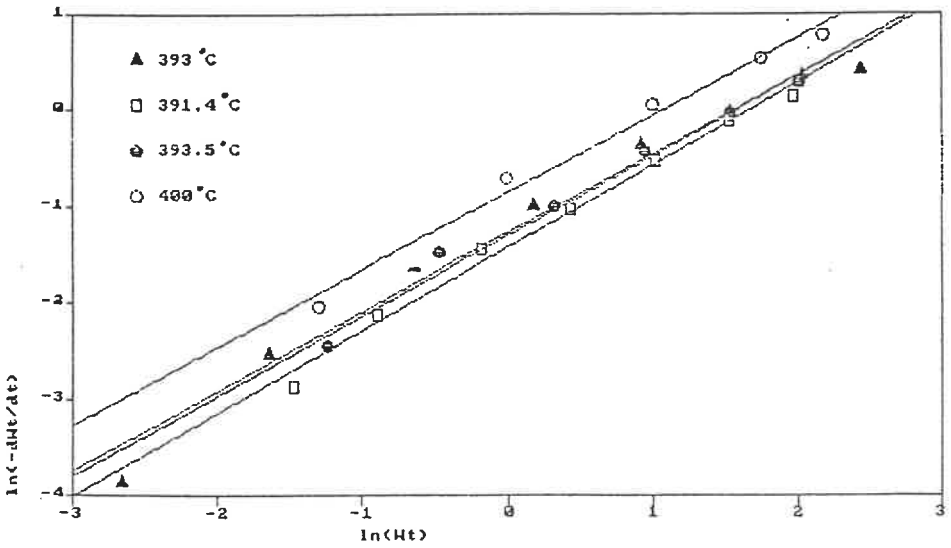

Fig. 22 $\ln(-dw_t/dt)$ versus $\ln(w_t)$ plots for PS isothermal degradation in helium atmosphere.

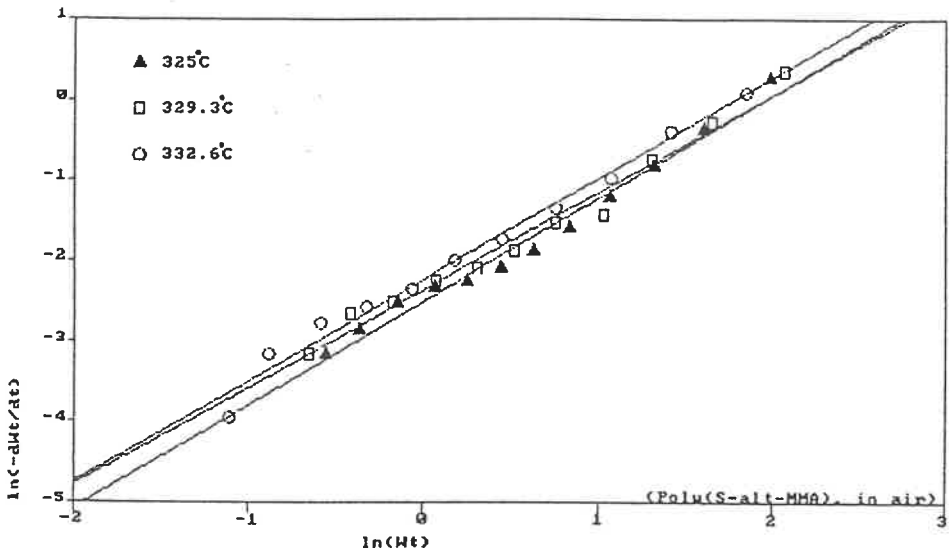

Fig. 23 $\ln(-dw_t/dt)$ versus $\ln(w_t)$ plots for poly(S-alt-MMA) isothermal degradation in air atmosphere.

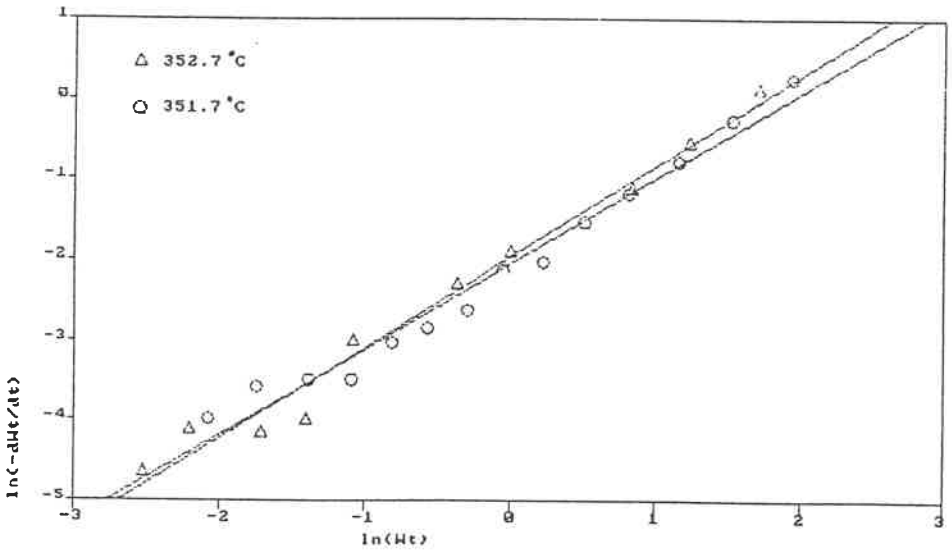

Fig. 24 $\ln(-dw_t/dt)$ versus $\ln(w_t)$ plots for poly(S-alt-MMA) isothermal degradation in helium atmosphere.

energy of activation of 273.2 kJ/mole.

Table 2

Activation energies (Ea) and reaction order (n)

calculated by isothermal method

Polymer	n	Ea(kJ/mole)	Atmosphere
polystyrene	0.7	198.3	air
polystyrene	0.8	254.8±17.2	helium
poly(S-alt-MMA)	1.2	108.1±6.7	air
poly(S-alt-MMA)	1.1	289.5	helium

In the case of the alternating copolymer, little work has been done. Hurduc[3] working in an atmosphere of air found that the activation energy was 232.2kJ/mole.

The values of polystyrene in Table 2 are in good agreement with those of other workers, including that of Hurduc[3], indicating that the experimental procedure is reliable. But the activation energy of poly(S-alt-MMA) in air listed in table 2 is 108.1kJ/mole, this is quite far from what published by Hurduc, 232.2 kJ/mole. The degradation of poly(S-alt-MMA) in inert gas has not been studied, no values can be compared with. In air atmosphere, Hurduc used Freeman and Carroll's differential method, and we used

isothermal method, both of these two are based on the same equation, Equ. 6, used the same simple model of $f(\alpha)$, Equ. 5. These gave us an idea: maybe Equ. 5 is not applicable in the degradation of poly(S-alt-MMA). Thus the degradation of poly(S-alt-MMA) was furthermore studied by multi-experimental comparison method with heating rates from 2 to 25° C/min, in air and argon atmosphere respectively, since multi-experimental comparison method does not depend on the form of $f(\alpha)$. There is no special reason that the inert gas was changed from helium to argon. Fig. 25 and Fig. 26 are log β versus 1/T curves of poly (S-alt-MMA) degradations in air and argon atmospheres, β is the heating rate, alpha (α) is the conversion, T is absolute temperature. Table 3 lists the calculation procedure (step by step explanation is written in Appendix IV), and Table 4 compares the activation energies obtained by different methods.

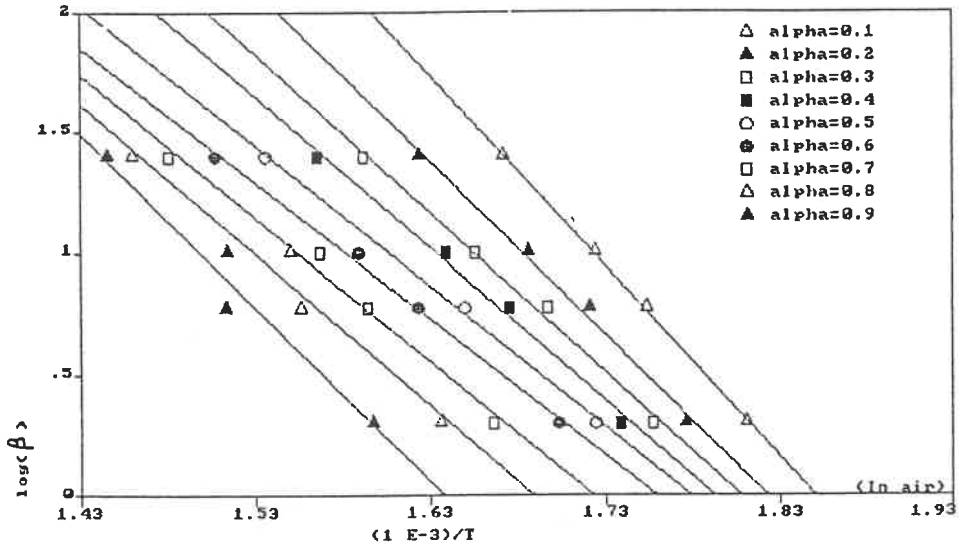

Fig. 25 Plots of log(β) versus 1/T in multi-experimental comparison method. Air atmosphere. Alpha (α) is the conversion.

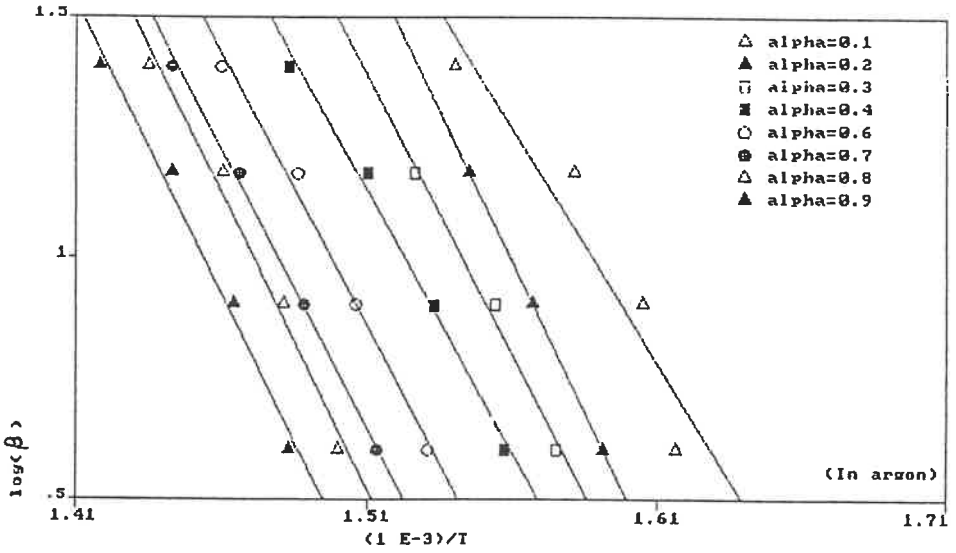

Fig. 26 Plots of log(β) versus 1/T in multi-experimental comparison method. Argon atmosphere.

Table 3

Ea of poly(S-alt-MMA) degradation evaluated by multi-experimental comparison method

Conversion α	slope 10^{-3}	$Ea_{approx.}$ (kcal/mole)	T (K)	Ea/RT (approx.)	Reevaluated constant	$Ea_{corrected}$ (kcal/mole)
Poly(S-alt-MMA) degrades in air						
0.3	-6.570	28.56	569	25.26	0.4685	27.86
0.4	-6.276	27.29	575	23.88	0.4701	26.53
0.5	-5.801	25.22	580	21.88	0.4732	24.36
0.6	-5.622	24.44	587	20.95	0.4751	23.51
0.7	-5.942	25.84	600	21.66	0.4737	24.92
0.8	-6.227	27.07	611	22.29	0.4724	26.19
Ea (in air, conversion 0.3-0.8):						25.56±1.45 kcal/mole = 107.0±6.1 kJ/mole
Poly (S-alt-MMA) degrades in argon						
0.2	-12.48	54.26	628.4	43.45	0.4540	54.62
0.3	-11.60	50.44	634.8	39.33	0.4560	50.55
0.4	-10.83	47.09	642.2	36.90	0.4580	46.98
0.6	-11.31	49.17	653.1	37.89	0.4562	49.26
0.7	-11.47	49.87	661.2	37.96	0.4561	49.97
0.8	-12.22	53.13	665.6	40.17	0.4558	53.27
0.9	-12.21	53.09	674.1	39.63	0.4560	53.20
Ea (in argon, conversion 0.2-0.9):						51.12±2.49 kcal/mole = 213.9±10.4 kJ/mole

Table 4

Activation energies of degradation of poly(S-alt-MMA) determined by different methods

Atmosphere	Method	Ea(kJ/mole)	Reference
air	differential	232.3	Hurduc[3]
air	isothermal	108.1±6.7	
air	multi-experimental	107.0±6.1	
helium	isothermal	289.5	
argon	multi-experimental	213.9±10.4	

In Table 4, each method gives a value different from others. We prefer the values determined by multi-experimental comparison method since this method do not depend on $f(\alpha)$, and the curves in Fig. 25 and Fig. 26 have good linearity.

Table 5 lists activation energies of all the S-MMA copolymer samples determined by multi-experimental comparison method. Block copolymer P-205-UV-A has higher activation energy than the other block copolymer P-210-D due to its higher average molecular weight.

Table 5

Ea's of thermal degradation of S-MMA copolymers evaluated by multi-experimental comparison method

Sample	PS %	copolymer	atmosphere	Ea(kJ/mole)
poly(S-alt-MMA)	50	alternating	air	107.0±6.1
P-210-D	38.4	block	air	128.9±9.9
P-205-UV-A	38.7	block	air	132.7±8.7
NAS	69.1	random	air	110.1±8.8
poly(S-alt-MMA)	50	alternating	argon	213.9±10.4
P-210-D	38.4	block	argon	211.4±9.1
P-205-UV-A	38.7	block	argon	249.1±14.2
NAS	69.1	random	argon	226.4±16.0

Fig. 27 and Fig. 28 show that PS degrades slower than poly(S-alt-MMA) in air and in helium atmosphere. This is in agree with the results given in Table 2 and Table 3, PS has higher activation energy than poly(S-alt-MMA). But Ea is not an absolute standard of stability, there are also some effect of kinetic factors. If the temperature at which the polymer loses half of its weight when heated in vacuum for 30 minutes is chosen as the characteristic temperature ($T_{1/2}$) for the thermal stability, $T_{1/2}$ is not

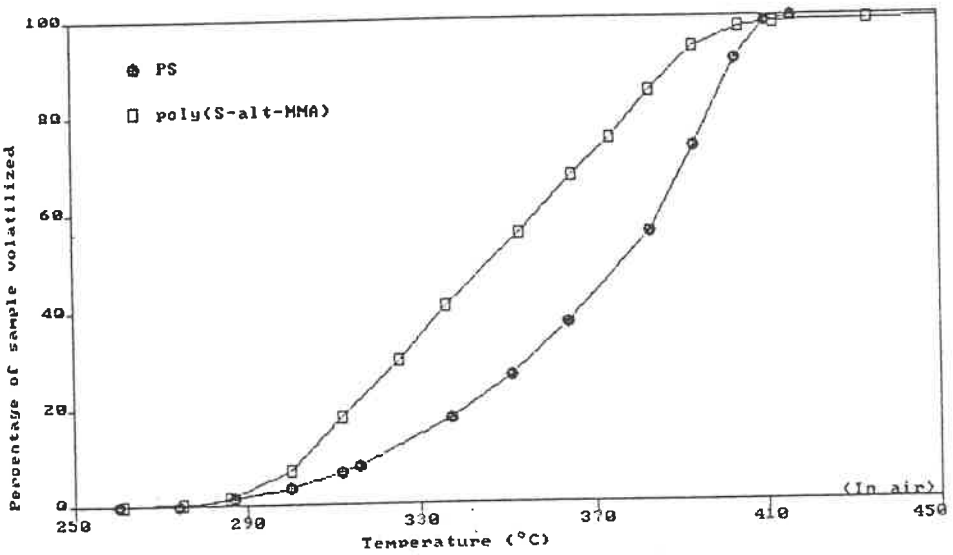

Fig. 27 Comparison of thermal degradation of PS and poly(S-alt-MMA) in air atmosphere. Weight loss vs. temperature. Heating rate 10°/min.

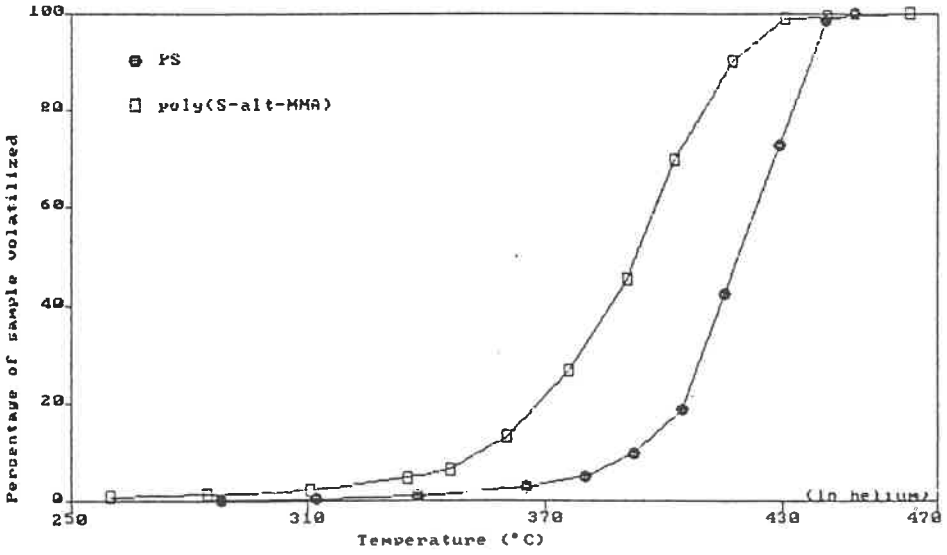

Fig. 28 Comparison of thermal degradation of PS and poly(S-alt-MMA) in helium atmosphere. Weight loss vs. temperature. Heating rate 10°/min.

essentially a linear function of activation energy. See Table 6[56].

IV. 2 THERMAL STABILITIES of S-MMA COPOLYMERS

Thermogravimetry was also used to study the thermal stability of polymers in this work.

First of all, Fig. 29 and Fig. 30 show us that S-MMA copolymers degrade faster in air than in inert gas. This is to be expected. The degradation of P-210 and NAS in air and in helium atmospheres gave the same kind of graphs as Figs. 29 and 30.

See Fig. 31 and Fig. 32, poly(S-alt-MMA) has about the same thermal stability as other copolymers in helium atmosphere. In air atmosphere, two reactions cause the loss of weight — degradation and oxidation, In this case, the alternating copolymer degrades faster than others.

In Fig. 32, the curves of P-205, P-210 and NAS are not complete at high conversion. Anyway, the relative stability at high conversion is not of interest because polymeric materials loose their physical properties, such as

Table 6[56]

Thermal degradation of polymers

Polymer	$T_{1/2}$ (°C)[1]	k_{350} (%/min)[2]	Monomer yield (%)	E_{act} (kJ/mol)
poly(tetrafluoroethylene)	509	0.000002	>95	339
poly(p-xylylene)	432	0.002	0	306
poly(p-phenylene methylene)	430	0.006	0	209
polymethylene	414	0.004	<0.1	301
poly(trifluoroethylene)	412	0.017	<1	222
polybutadiene	407	0.022	2	260
polyethylene (branched)	404	0.008	<0.025	264
polypropylene	387	0.069	<0.2	243
poly(chlorotrifluoroethylene)	380	0.044	27	239
poly(β-deuterostyrene)	372	0.14	39	234
poly(vinylcyclohexane)	369	0.45	0.1	205
polystyrene	364	0.24	40	230
poly(α-deuterostyrene)	362	0.27	68	230
poly(m-methylstyrene)	358	0.90	45	234
polyisobutylene	348	2.7	20	205
poly(ethylene oxide)	345	2.1	4	193
poly(α,β,β-trifluorostyrene)	342	2.4	7.4	268
poly(methyl acrylate)	328	10	0	142
poly(methyl methacrylate)	327	5.2	>95	218
poly(propylene oxide) (isot.)	313	20	1	147
poly(propylene oxide) (atact.)	295	5	1	84
poly(α-methylstyrene)	286	228	>95	230
poly(vinyl acetate)	269	–	0	71
poly(vinyl alcohol)	268	–	0	–
poly(vinyl chloride)	260[3]	170[3]	0[3]	134[3]

[1] Temperature at which the polymer loses 50% of its weight, if heated in vacuum for 30 minutes.
[2] Rate of volatilization (weight loss) at 350°C.
[3] Determined from the loss of HCl.

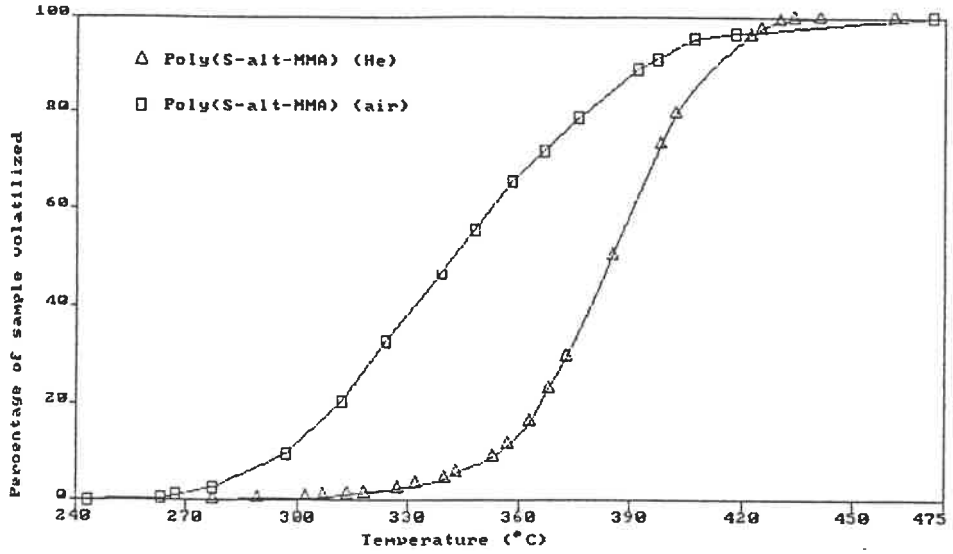

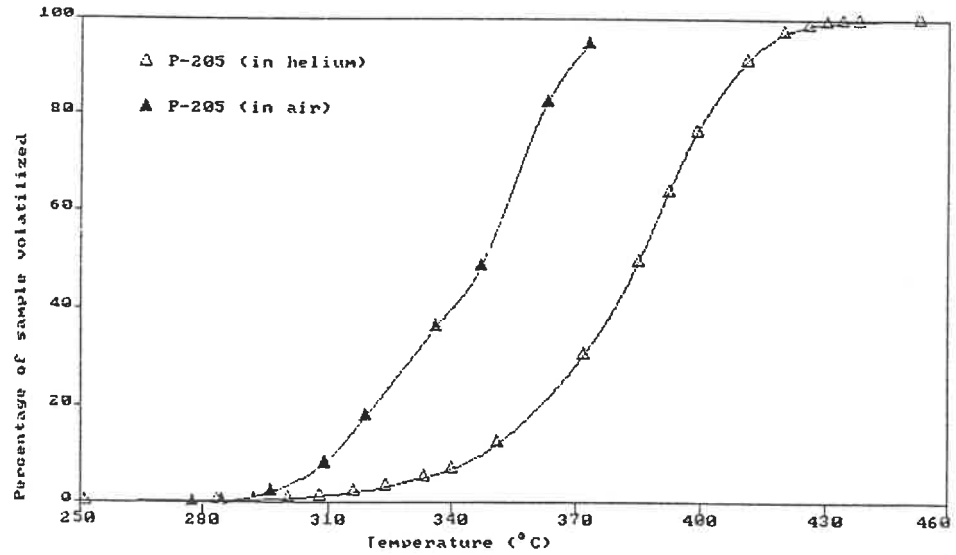

Figs. 29, 30 Degradations of S-MMA copolymers. Heating rate 10 °C/min. Weight loss vs. temperature.

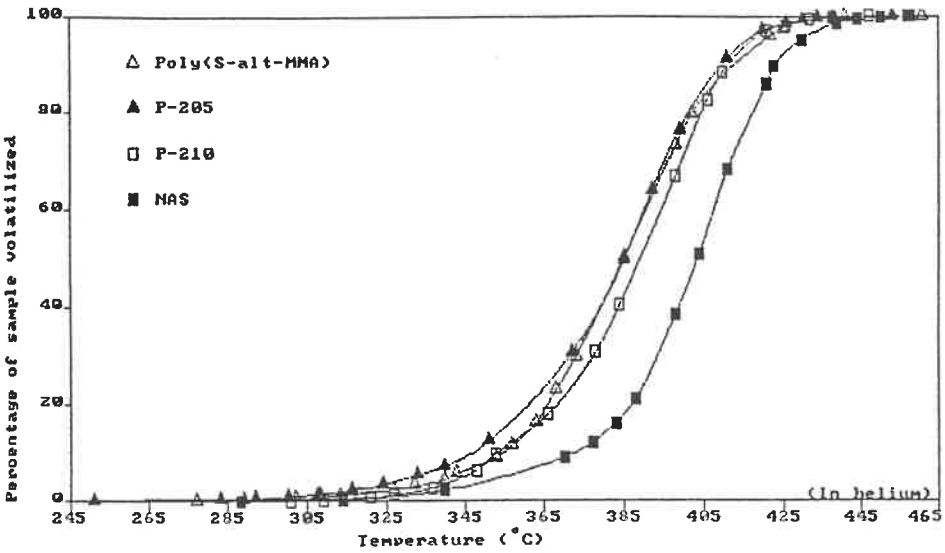

Fig. 31 Degradation of S-MMA copolymers in helium atmosphere under 10°C/min heating rate, weight loss vs. temperature.

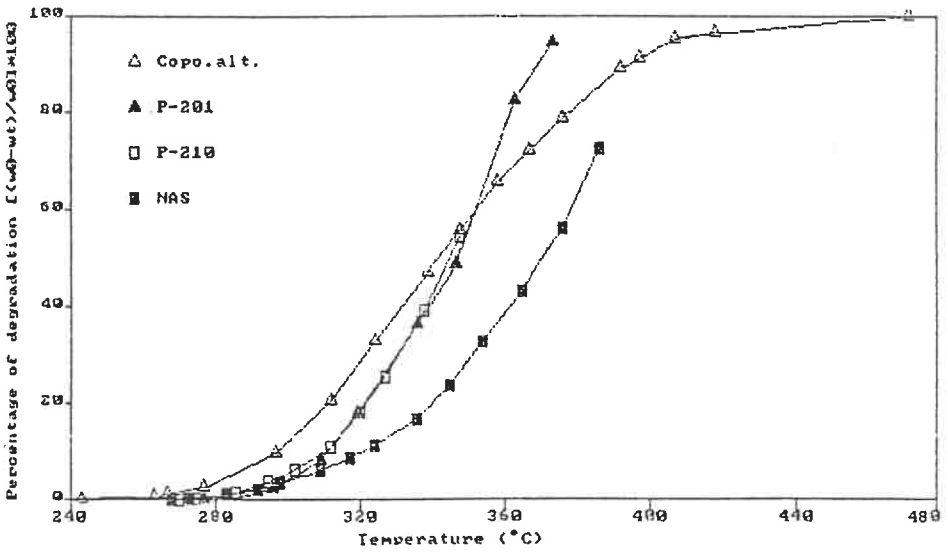

Fig. 32 Degradation of S-MMA copolymers in air atmosphere under 10°C/min heating rate, weight loss vs. temperature.

mechanical properties, colour and appearance, at very low even zero conversion.

In Figs. 31 and 32, NAS is always the most stable one, because it contains higher level of styrene, 69.1%. The others contain 40%, 50% styrene. PS is more thermally stable than PMMA, see Fig. 33 and Fig. 34.

Next, the thermal stabilities of PS-PMMA blend and S-MMA copolymers in air atmosphere were compared. In Fig. 35, the "predicted PS38.6% + PMMA61.4%" curve is constructed from the weight losses of the constituent polymers when degraded alone, i.e., degradation of mixture of PS 38.6% + PMMA 61.4% as if there is no interaction between these two polymers. The "mixture of PS(38.6%) + PMMA(61.4%)" curve is the experimental curve of PS-PMMA powder mixture. The Figure shows that when PS and PMMA are mixed together, the stability at low conversion is improved and at high conversion is deteriorated with respect to the pure homopolymers. Because at low temperature, the weight loss is mainly caused by chain end initiated degradation of PMMA[57-58], the presence of PS retards the degradation of PMMA as the resonance favors the phenyl rings on PS chains over the double bonds at PMMA's chain ends for the free electron, thus the chain end initiated degradation is largely reduced; at high temperature, random chain scission

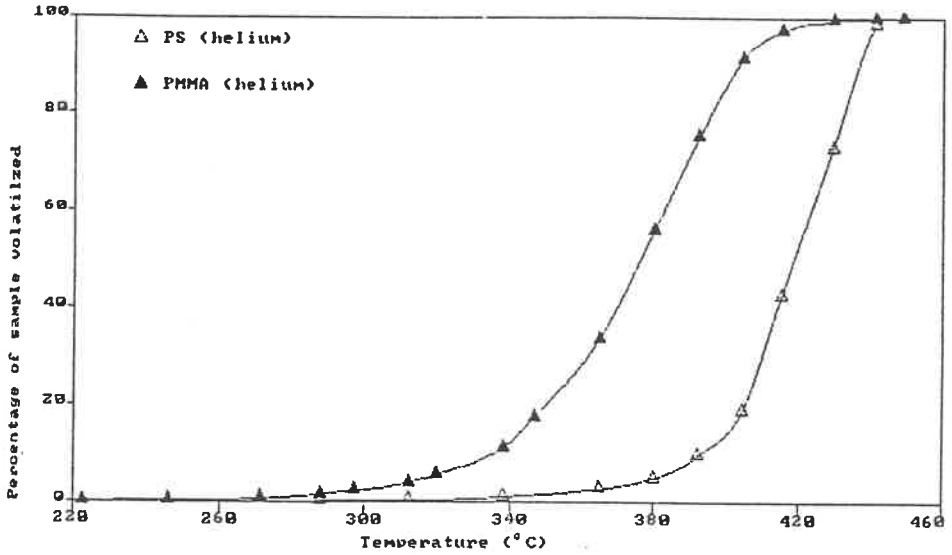

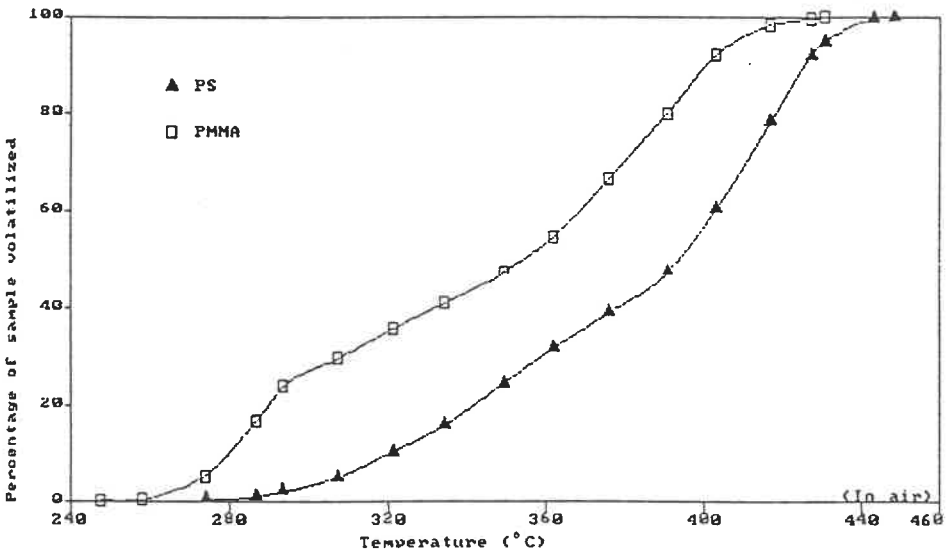

Figs. 33, 34 Degradations of PS and PMMA in helium and air atmospheres under 10°C/min heating rate. Weight loss vs. temperature.

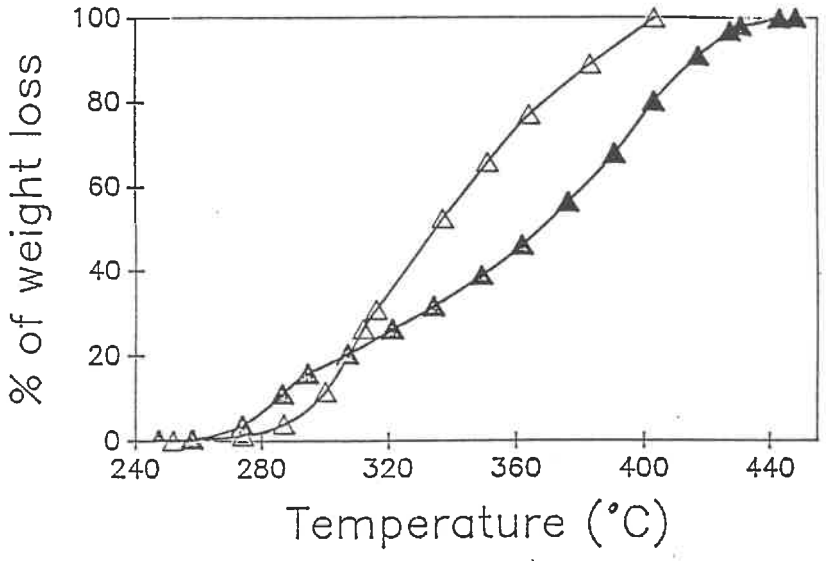

Fig. 35 Degradation of PS-PMMA blend. Weight loss vs. temperature. The heating rate was 10 °C/min, in air atmosphere.
Δ : mixture of 38.6% PS with 61.4% PMMA;
▲ : predicted results for the same mixture.

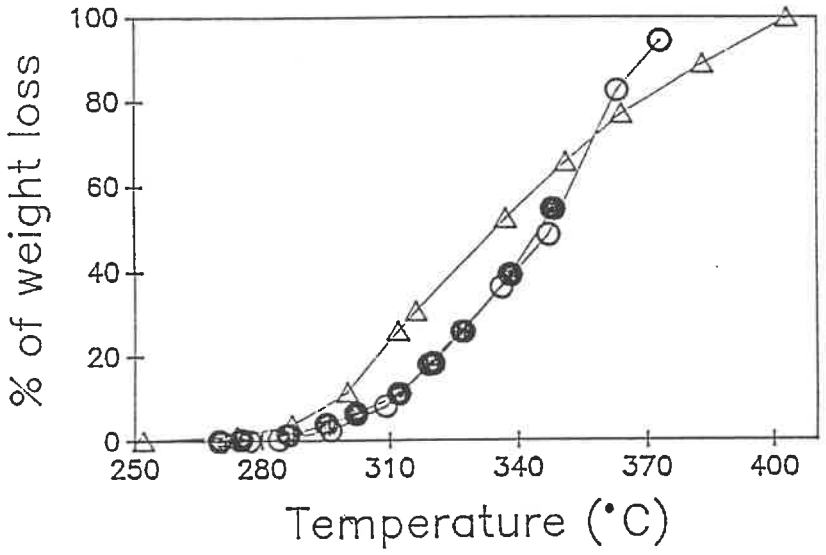

Fig. 36 Degradation of S-MMA block copolymers and PS-PMMA blend. Weight loss vs. temperature. Air atmosphere, heating rate 10°C/min.
O : P-205, styrene 38.7% + methyl methacrylate 61.3%;
● : P-210, styrene 38.4% + methyl methacrylate 61.6%;
Δ : mixture of 38.6% PS with 61.4% PMMA.

and depolymerization happen to both PMMA and PS, the segments of PMMA accelerate the decomposition of PS.

Fig. 36 shows that the S-MMA block copolymers have the same phenomena (improved stability at low conversion and deteriorated stability at high conversion) more obvious than PS-PMMA mixture. It is the same for S-MMA alternating and random copolymers, see Fig. 37. The disproportionately large increase in stability with increasing styrene content has also been observed by Grassie, Farish[59] and McNeill[60]. Grassie and Farish' explanation is that copolymers of this pair of monomers would be expected, in view of the calculation of Bevington et al[61], to have scarcely any terminal unsaturated methyl methacrylate end since the cross termination reaction is favoured in the polymerization process and occurs almost exclusively by radical combination rather than disproportionation. This explanation is reasonable for free radical mechanism polymerized random copolymers and S...S-M...M-S...S type block copolymers. McNeill's explanation is that the radical pair resulting from an initial scission of the chain at temperature around 270 to 320°C (the range at which PMMA starts to degrade) depolymerize only as far as the nearest styrene unit. The styryl radical ends thus obtained do not depolymerize to give volatile products at this temperature, and may possibly recombine or disproportionate. It is only in the

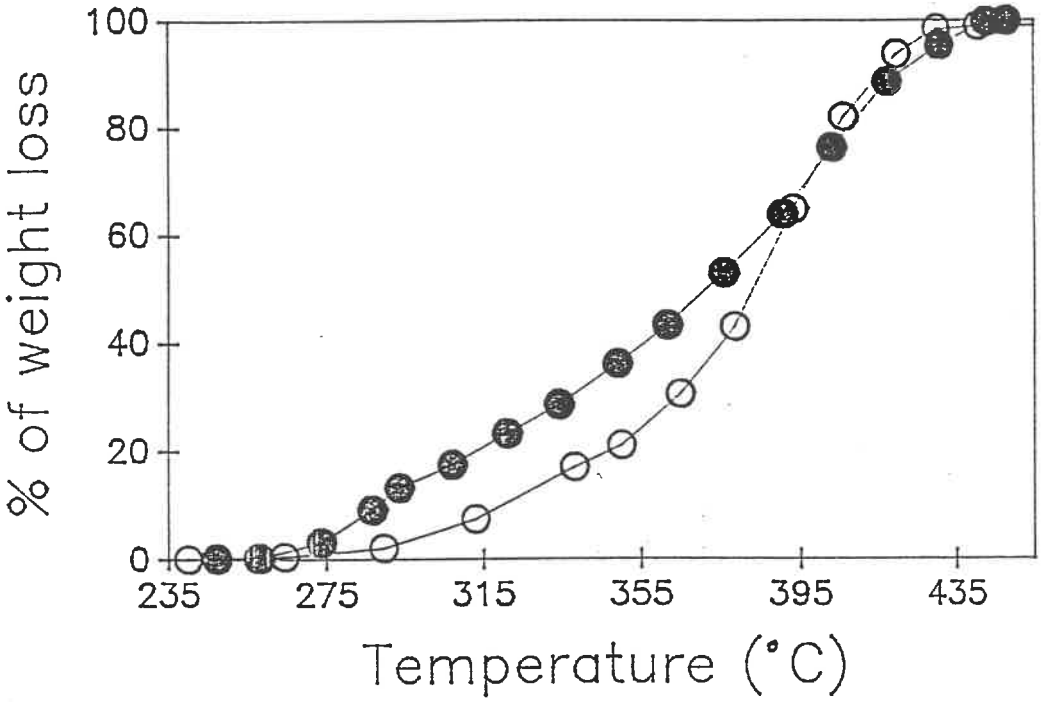

Fig. 37 Degradation of poly(S-alt-MMA), weight loss vs. temperature, heating rate 10°C, air atmosphere.
O : poly(S-alt-MMA);
● : predicted results for a 50/50 of PS/PMMA mixture.

temperature range for breakdown of polystyrene that depolymerization occurs. Neither of these explanation elucidates the stabilizing effect of PS in PS-PMMA blend.

IV. 3 STABILIZATION of S-MMA COPOLYMERS

As poly(S-alt-MMA) was polymerized at presence of zinc chloride, it is possible that the thermal stability of poly(S-alt-MMA) is affected by zinc ions Zn^{++}. Following this idea, Irganox MD-1024, a metal deactivator/antioxidant, and Irganox 1010, an antioxidant, were added respectively to poly(S-alt-MMA). The chemical structures of these two stabilizers are shown in Appendix V. Both of them are hindered phenols, the only difference between them is that MD-1024 has a 1,2-diazanediyl structure (-NHNH-) which deactivate metals. Figs. 38 and 39 shows that Irganox MD-1024 is indeed a better stabilizer than Irganox 1010, this result proves the hypothesis that the zinc ions do catalyze the degradation.

The thermal degradation of poly(S-alt-MMA) without zinc needs more studies.

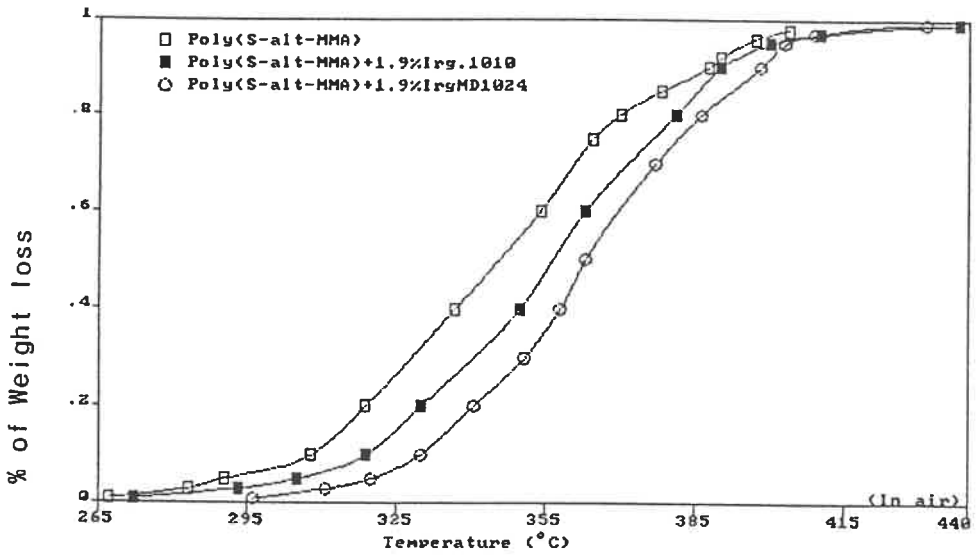

Fig. 38 Weight loss of poly(S-alt-MMA) samples with and without stabilizers versus temperature. The heating rate was 10°C/min, air atmosphere.

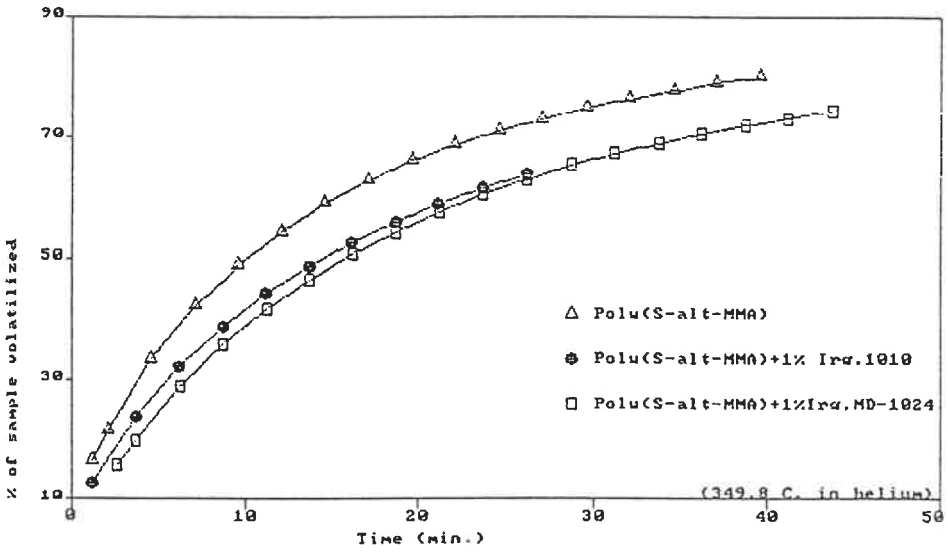

Fig. 39 Weight loss of poly(S-alt-MMA) samples with and without stabilizers versus degradation time at 349.8°C in helium atmosphere.

For the stabilization of PS, PMMA and their copolymers, phenols[62-64], phosphite[65,66], mercaptan in the presence of an alkali [67], dialkyltin maleates[68] and amine[64] have been used by different workers. Hindered phenols are primary antioxidant (see Section II. 2), they were selected in our work because of the presence of zinc chloride.

For polymers containing metal, Irganox 1010 is suggested to be used together with Irganox MD-1024 by Ciba Geigy Co.. Figs. 40-43 demonstrate that more stabilizers does not imply necessarily an increased stability, no matter one stabilizer is used alone or two stabilizers are combined together. In fact, too much stabilizers may reduce the stabilizing effect, see Figs. 42 and 43. It has been found that under certain conditions, antioxidant can also initiate oxidation, as published by Shlyapnikov[69].

Fig. 42 shows that 0.5% Irganox 1010 and 0.5% Irganox MD-1024 give the best stabilization for poly(S-alt-MMA) while only 0.2% each stabilizer is enough for P-210, see Fig. 43. This is because there have to be enough Irganox MD-1024 for the zinc ions remaining in poly(S-alt-MMA).

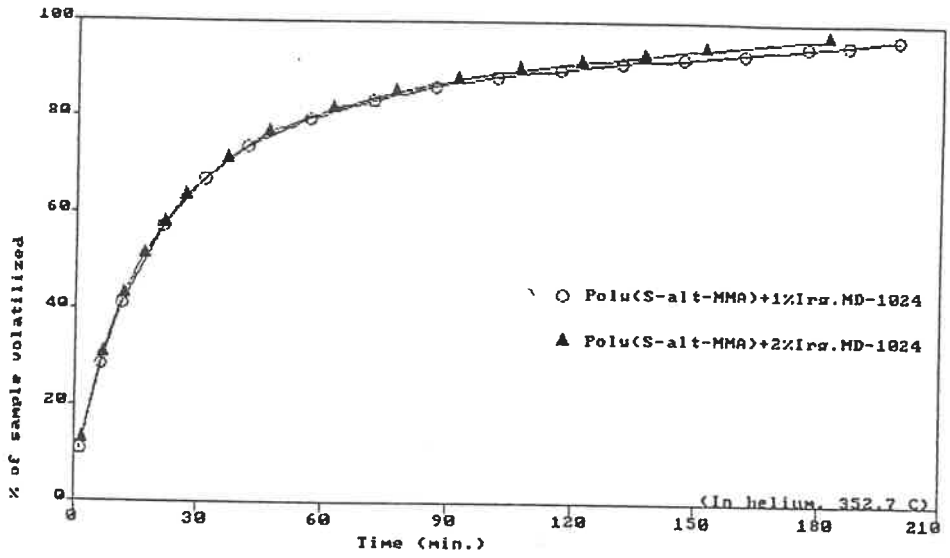

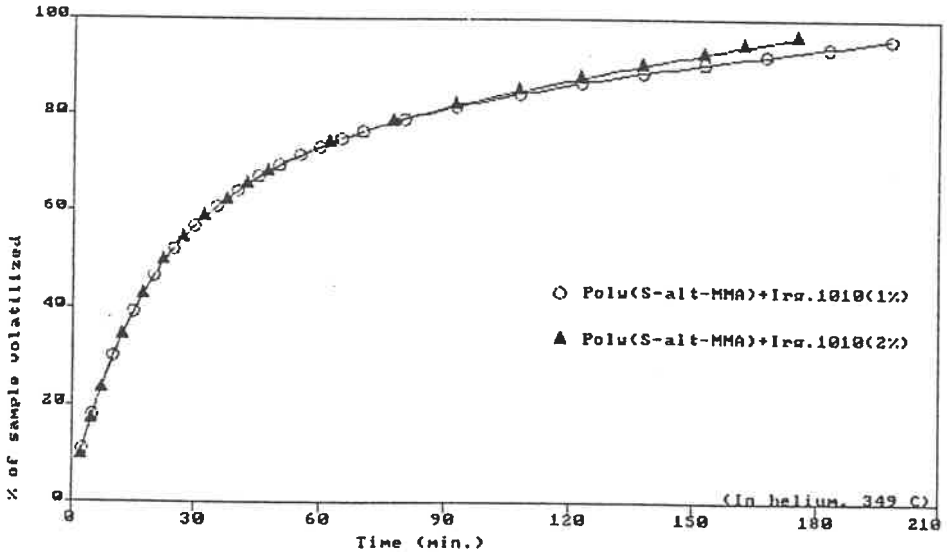

Figs. 40, 41 Weight loss of stabilized poly(S-alt-MMA) sample versus degradation time under constant temperature, helium atmosphere.

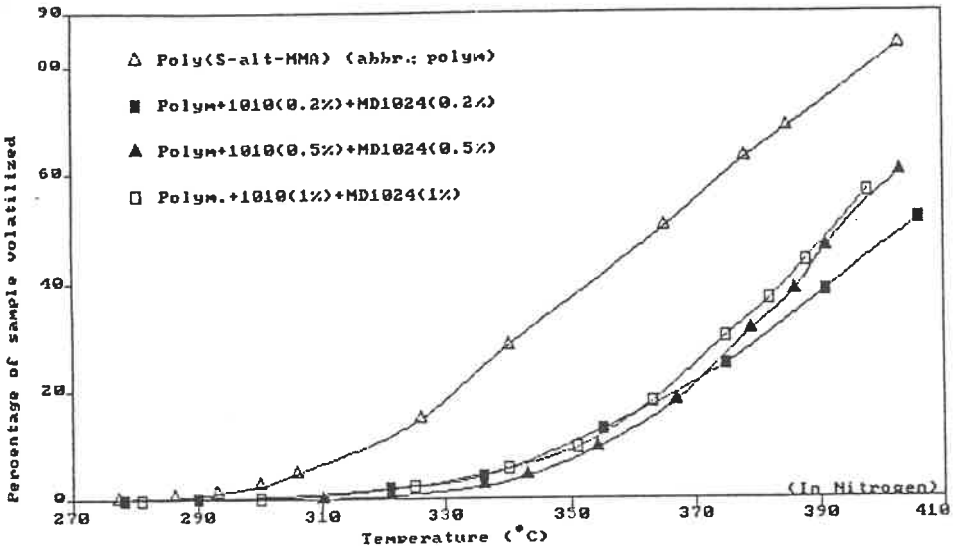

Fig. 42 Stabilization of poly(S-alt-MMA) by Irganox 1010 and Irganox MD-1024. Weight loss vs. temperature. 10°C/min heating rate, nitrogen atmosphere.

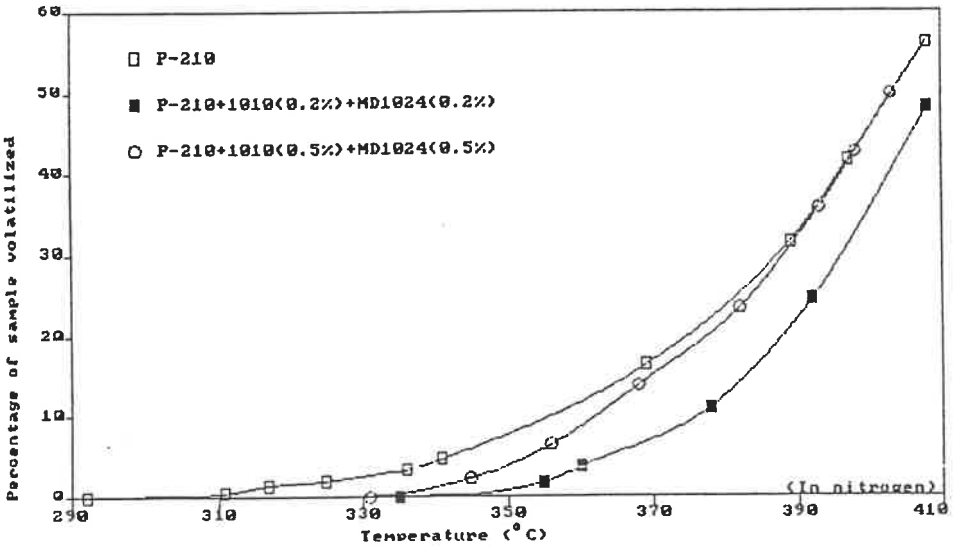

Fig. 43 Stabilization of S-MMA block copolymer P-210 by Irganox 1010 and Irganox MD-1024. Weight loss vs. temperature, nitrogen atmosphere.

IV. 4 MECHANICAL PROPERTIES of S-MMA COPOLYMERS, PS and PMMA

As poly(S-alt-MMA) is a quite new polymer, up to what we know, its mechanical properties has not been examined. And as mentioned in section II. 3, this is one of the most important information of a material. Therefore, in this work, the mechanical properties of this alternating copolymer were tested. For comparing, mechanical properties of S-MMA block copolymers P-205-UV-A and P-210-D, S-MMA random copolymer NAS, homopolymers PS and PMMA were also examined. Results are listed in Table 7.

Table 7

Mechanical Properties

Polymer samples	Tensile modulus E(MPa)	Tensile strength σ_b(MPa)	Ultimate strain ϵ_b(%)
poly(S-alt-MMA)	2275±77	50.13±0.67	3.3±0.0
P-205-UV-A	2054±76	53.51±0.5	3.4±0.5
P-210-D	2491±26	51.09±1.48	3.5±0.1
NAS	2045±106	42.88±1.90	2.9±0.2
PS	2115±26	31.98±0.96	2.3±0.1
PMMA	2261±192	49.31±0.86	4.8±0.4

It has been found that stress-strain tensile properties of a polymer is the function of its average molecular weight and polydispersity[23,70,71], higher its molecular weight or polydispersity is, bigger its tensile strengths and ultimate strains are. See Figs. 44 and 45.

P-205 and P-210 are block copolymers of different average molecular weights, the tensile strength of P-205 is higher than that of P-210, because P-205 has higher molecular weight than P-210, and their polydispersities are the same. The ultimate strains of P-205 and P-210 are about the same, since at their molecular weight, the ultimate strain has already reached the level off region. The random copolymer, NAS, has poorer tensile properties than P-210 and P-205, although its average molecular weight is between P-210 and P-205. Also, poly(S-alt-MMA) has higher number average molecular weight and polydispersity than those two block copolymers, but does not have better tensile properties than them. Hence, for S-MMA copolymers, block copolymer has the strongest tensile properties. These suggest that not only the molecular weight and polydispersity of a copolymer is important for its mechanical properties, but also the molecule arrangement of various constituents of this copolymer.

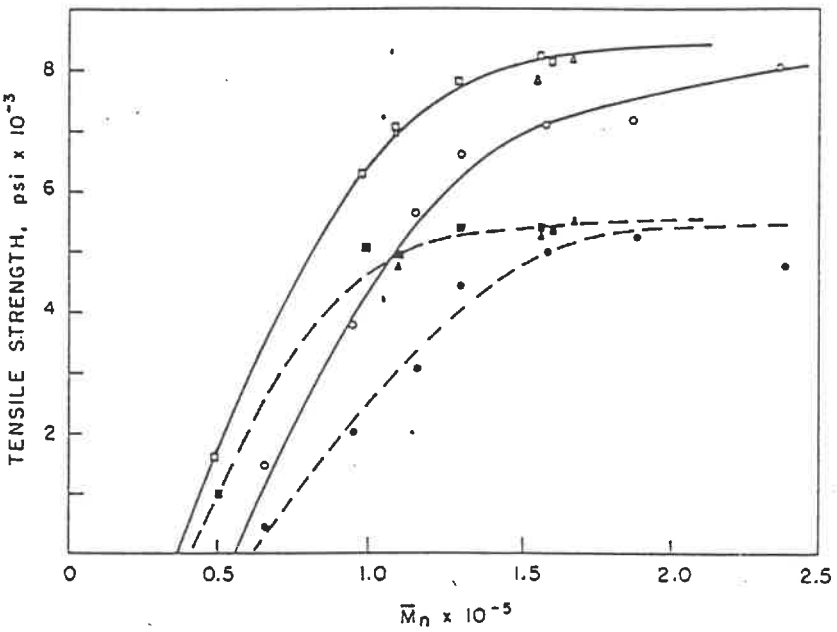

Fig.44 A plot of tensile strength against number-average molecular weight for (○, ●) anionic, (□, ■) isothermal and (△, ▲) thermal polystyrene. Open symbols for injection-molded and filled symbols for compression-molded specimens.

Polydispersity of anionic PS is about 1.1, of isothermal PS is about 2.0, and of thermal PS is about 2.4.

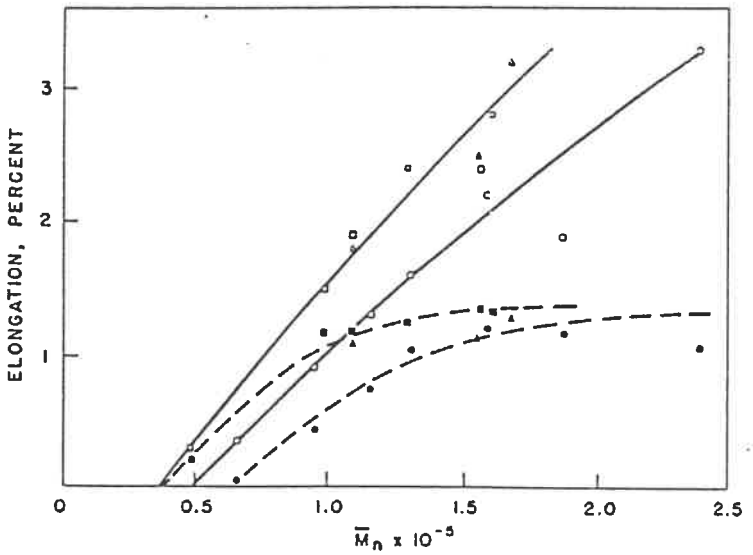

Fig.45 A plot of elongation against number-average molecular weight for (○, ●) anionic, (□, ■) isothermal, and (△, ▲) thermal polystyrene. Open points for injection-molded and solid points for compression-molded specimens.

IV. 5 GLASS TRANSITION TEMPERATURES

Like mechanical property, glass transition temperature is also a very important data for engineers and scientist, it determines the polymer's properties such as the transition from solid to rubber behavior, the creep rate, the rheological characteristics, the crystallization rate and the toughness. Thus, the glass transition temperatures of the polymers samples were measured by DSC and the results are presented in Table 8.

Table 8

Glass transition temperatures

Sample	% PS	T_g (°C)	Remarks
poly(S-alt-MMA)	50	107.5±0.3	alternating copolymer
P-205	38.7	102.5±0.2	block copolymer
P-210	38.4	100.8±0.1	block copolymer
NAS	69.1	97.7±0.3	random copolymer
PS	100.0	101.2±0.5	homopolymer
PMMA	0.0	89.4±0.1	homopolymer

In Table 8, the Tg of poly(S-alt-MMA) is higher than

that of the block and random copolymers. The molecular weight of poly(S-alt-MMA) is bigger than others, see Table. 1. Fox et al.[72,73] have proposed an equation to relate number average molecular weight with glass transition temperature:

$$Tg = Tg^{\infty} - K/\bar{M}n \qquad (53)$$

where Tg^{∞} is the Tg at infinite molecular weight, K a constant of each polymer, it has value of $1.7*10^5$ for PS[72] and $2.1*10^5$ for PMMA[74]. According to Equ. 53, T_g's of other polymers were calculated as if they have the same number average molecular weight as poly(S-alt-MMA), the results are listed in Table 9.

Table. 9

Corrected glass transition temperatures, Mn = $2.9x10^5$

Sample	% PS	T_g (°C)	Remarks
poly(S-alt-MMA)	50	107.5	alternating copolymer
P-205	38.7	103.4	block copolymer
P-210	38.4	103.2	block copolymer
NAS	69.1	98.7	random copolymer
PS	100.0	102.0	homopolymer
PMMA	0.0	95.9	homopolymer

Table 9 shows that for S-MMA copolymers, the alternating copolymer has the highest glass transition temperature, after is the block copolymer, and the random copolymer has the lowest Tg. In fact, Tg of the random copolymer NAS follows well the empirical formulas which has been found to apply fairly well in many cases[75]:

$$\frac{1}{Tg} = \frac{w_1}{Tg_1} + \frac{w_2}{Tg_2} \qquad (54)$$

where Tg_1 and Tg_2 are the glass transition temperatures in degree Kelvin of pure homopolymers 1 and 2 respectively. The corresponding weight fractions are w_1 and w_2. And the glass transition temperature of the copolymer is Tg. According to Equ. 54, the predicted Tg of NAS is 100.1°C, and the value in Table 9 is 98.7°C, 1.4°C difference. Comparing with the work of Beevers and White[76], they found that for acrylonitrile-methyl methacrylate copolymers, block copolymers have glass transition temperatures intermediate between those of the parent polymers, while the glass temperature of the random copolymers for the most part fall below the glass temperature of polyacrylonitrile —— the homopolymer who has the lower Tg.

Another thing worth mention is that the T_g's of P-210

and P-205 in Table 9 are essentially the same, 103.2°C and 103.4°C. As we have known that the only difference between P-210 and P-205 is the molecular weight, this result is in good agreement with Fox et al.'s work.

IV. 6 POSSIBILITY for S-MMA COPOLYMERS to Be COMPATIBILIZERS for PS-PMMA BLEND

Polystyrene-polymethyl methacrylate system has been proved to be incompatible by measuring ultrasonic velocities in solids[44] and solutions[45], measuring glass transition temperatures[77-80], and observation of phase separation in solutions and films[30,78-84]. Therefore, a compatibilizer for this system will be very useful. Thus the possibility for S-MMA copolymers to be compatibilizers were tested.

PS-PMMA blends were made with Brabender, different criteria of compatibility were examined. Also, styrene-methyl methacrylate block copolymer P-210-D and poly(S-alt-MMA) were added at 10% entire weight of polymers in order to see if they have any compatibilizing effect for PS-PMMA system.

There are three copolymers provided by Richardson

Co., NAS, P-210-D and P-205-UV-A. NAS is a random copolymer, P-205 and P-210 are block copolymers of the same composition, see Table 1. They have the same NMR spectra, the only difference between P-205 and P-210 is the molecular weight, $9.1*10^4$ for P-205, and $5.4*10^4$ for P-210. It has been believed that block and graft copolymers are preferable compatibilizers, they can locate easily at the interface of the two phases. And in the case where a blend contains a volume fraction x of polymer A as spherical particals of radius R in a matrix of polymer B, see Fig. 46, the equation to estimate the amount of the block copolymer of molecular weight M required to saturate all of the interface in this blend is[85]

$$\frac{\text{mass of block copolymer}}{\text{original volume of blend}} = 3xM/aRN \qquad (55)$$

where N = Avogadro's number;

a = a constant depending on the system.

According to Equation 55, the amount of the block copolymer needed to saturate all the interfaces in a blend is in proportion to the molecular weight of the block copolymer. Consequently for the same kind of block copolymer, the one of smaller molecular weight is preferred. If there are different kinds of block and graft copolymers,

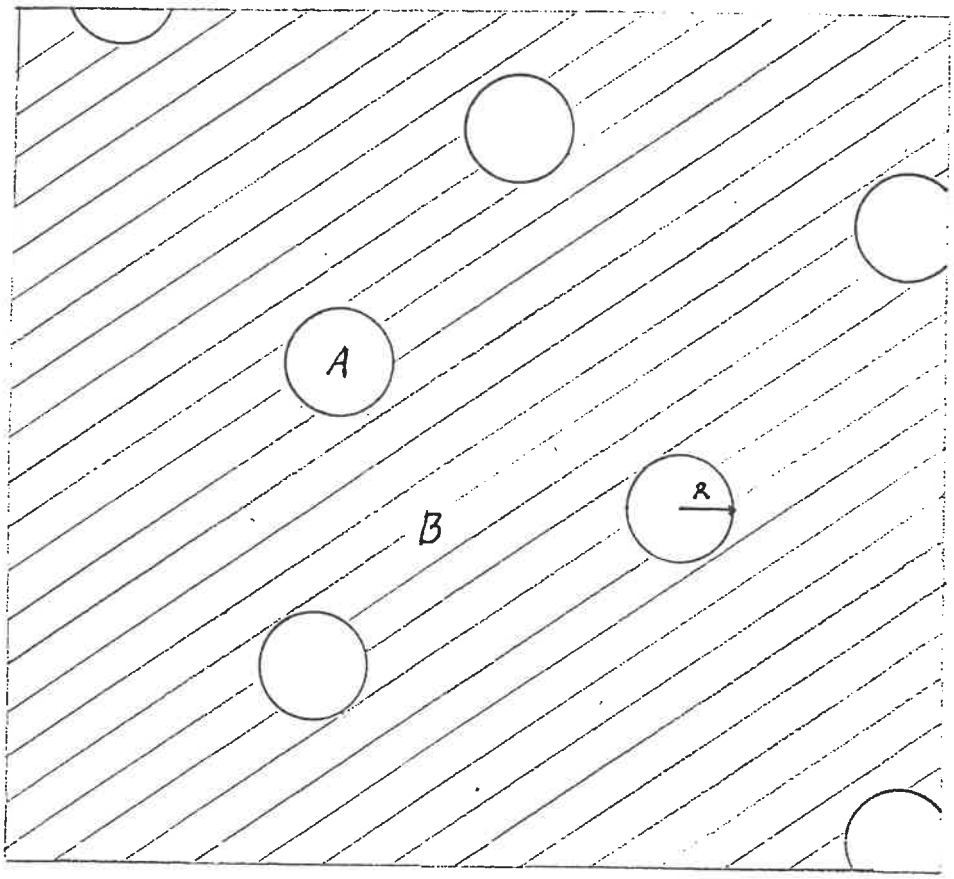

Fig. 46 Spherical particles of polymer A in the matrix of polymer B.

the one with molecular weights of segments bigger than or compatible to the corresponding homopolymers will be the one to have the best compatibilizing effect. Then, in our experiment, only P-210 was chosen from the three commercial copolymers as an potential compatibilizer, since it is a block copolymer, and its molecular weight is smaller than that of P-205. Although it has been found that block and graft copolymers are better compatibilizers, we tested the possibility for poly(S-alt-MMA) to be a compatibilizer as well since this copolymer is the main object of my project.

IV.6.A Optical Clarity

The appearance of PS-PMMA blends in the proportion of 10% to 80% PS are not transparent. It is in agreement with literatures[30,79-81]. It means that PS and PMMA are not compatible in the range of 10% to 80% PS. The adding of block copolymer P-210-D and poly(S-alt-MMA) did not change the clarity.

IV.6.B Dynamic Mechanical Properties

The dynamic mechanical properties of PS-PMMA blend without and with block copolymer P-210-D are presented in Fig. 47. Unfortunately, as the highest dissipation factor tgδ the Rheovibron can measure is 1.7, the glass transition peaks could not be measured entirely. The same phenomenon has been observed by others, see Fig. 48[81]. Thus, this very efficient method could not be used in our case. One thing can be seen from Fig. 47, the beginning of the glass transition peak of blend shifts a little when P-210-D is added. Although the shift is small, it does indicate that P-210-D has some compatibilizing effect on PS and PMMA blend.

The blend containing P-210-D has an extra second transition at 84°C. More study is needed to interpret this peak.

IV.6.C Differential Scanning Calorimetry

Since the change of Tg according to the compatibility of the system can not be detected by Rheovibron, DSC was employed. Table 10 lists the results of DSC, where T_g is the glass transition temperature, and T_f is the extrapola-

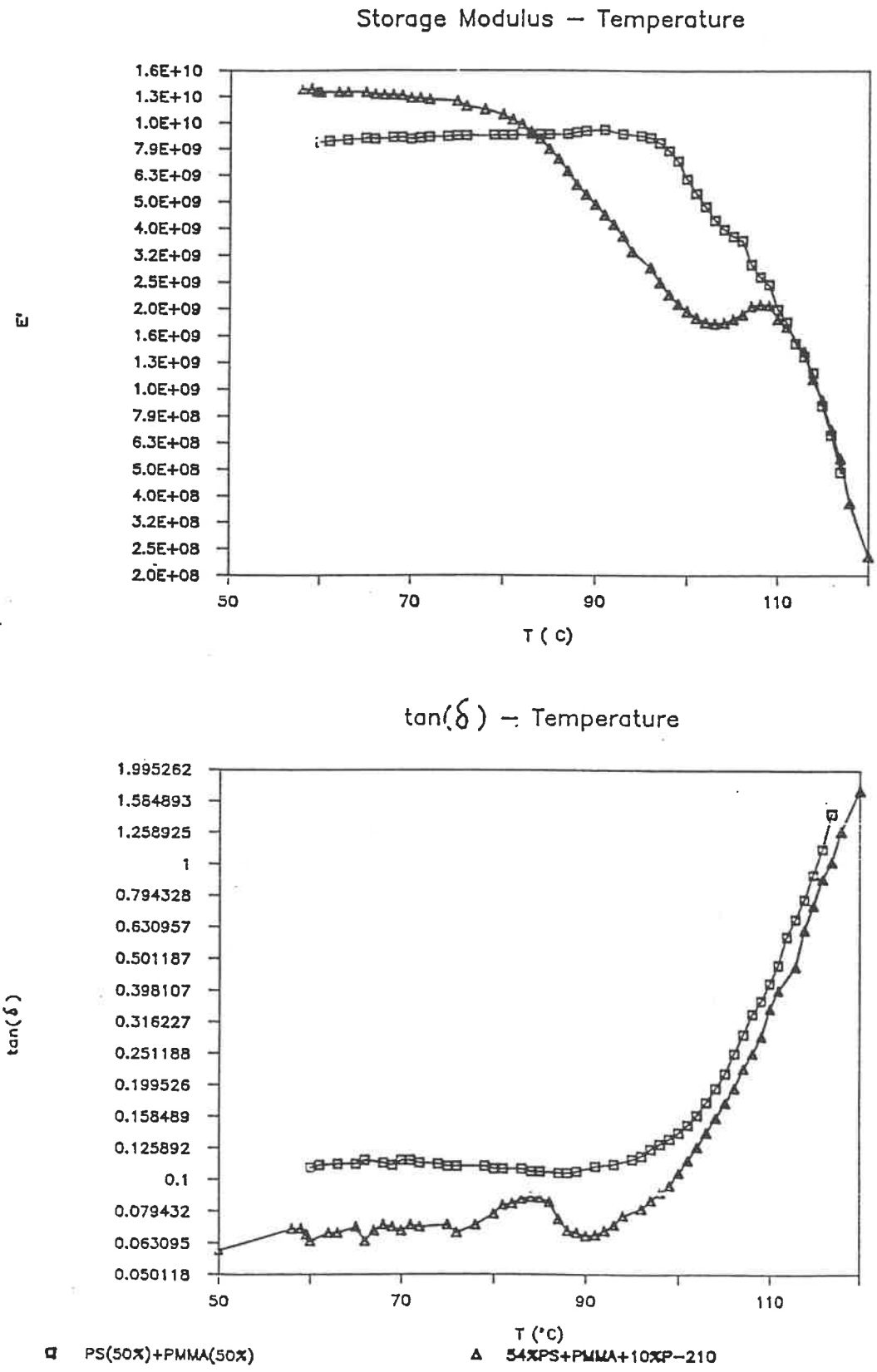

Fig. 47 Dynamic mechanical properties of PS-PMMA blend with and without block copolymer P-210 at 110 Hz.

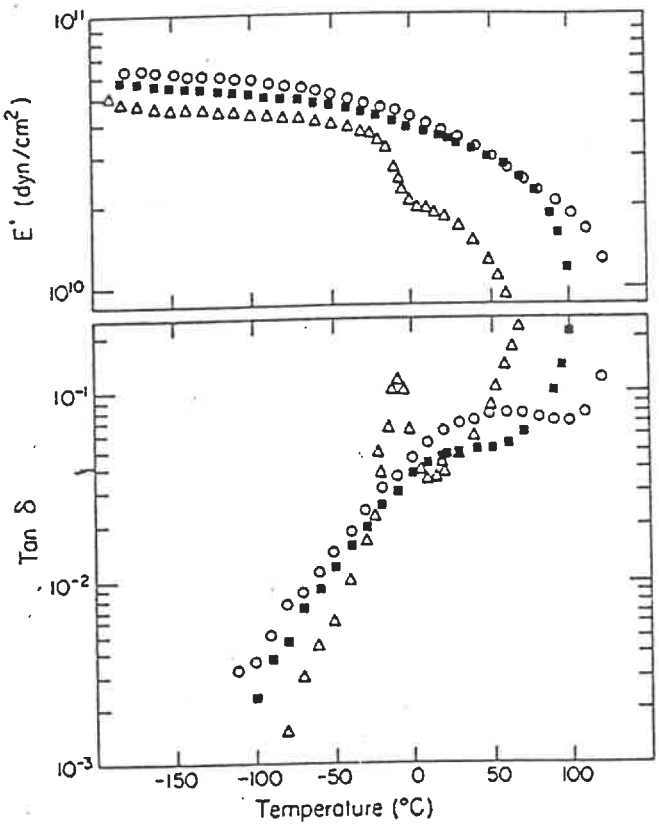

Figure 48 Dynamic mechanical properties of PMMA and blends of PS-600 with PMMA at 11 Hz. (○) PMMA; (■) 20 wt% PS-600 in PMMA; (△) 50 wt% PS-600 in PMMA.

ted onset temperature, see Fig. 19.

As $2(T_g - T_f)$ is the range of the transition region, it can be seen from Table 10 that all the blends have only one T_g, but the transitions are broadened. Since the T_g of PS and that of PMMA are quite close (11.8°C apart), the double T_g merge in only one. This is a very ordinary phenomenon when two Tg's are less than 20°C apart[19].

Comparing the glass transition regions of PS-PMMA blends with and without copolymers, the copolymers do not narrow the transition region.

The Tg transition region of blends mixed with Brabender are somewhat less broad than those of the powder mixtures, although not significantly, it does gave us an idea that at least some interdifusion takes place while PS and PMMA were fusion blended.

Table 10

Glass transition temperatures of polymers and blends

Sample	% PS	T_f (°C)	T_g (°C)	$2(T_g-T_f)$	Remarks
PS	100	96.0±0.4	101.2±0.5	10.4	
PMMA	0	85.4±0.4	89.4±0.1	8.0	
poly(S-alt-MMA)	50	106.2±0.7	107.5±0.3	2.6	
P-205	38.7	96.5±0.4	102.5±0.2	12.0	
P-210	38.4	94.9±0.3	100.8±0.1	11.8	
NAS	69.1	94.5±1.5	97.7±0.3	6.4	
PS+PMMA	38.6	85.9±0.1	93.8±0.2	15.8	powder mixture
PS+PMMA	40	88.2±1.2	95.5±0.7	14.6	mixed with Brabender
PS+PMMA(54%)+poly (S-alt-MMA)(10%)	36	85.6±0.5	95.6±0.3	20.0	powder mixture
PS+PMMA(54%)+poly (S-alt-MMA)(10%)	36	88.4±0.6	97.5±0.1	18.2	mixed with Brabender
PS+PMMA(54%)+ P-210-D(10%)	36	84.7±0.5	94.8±0.4	20.2	mixed with Brabender
PS+PMMA(54%)+ NAS(10)	36	85.4±0.7	94.9±0.3	19.0	mixed with Brabender

Chapter V

CONCLUSIONS

1. Thermal degradation of poly(S-alt-MMA) cannot be simply expressed by Equ. 6. The Ea's of S-MMA copolymers are measured. The activation energy of poly(S-alt-MMA) was found to be 107.0 kJ/mole when tested in air atmosphere and 213.9 kJ/mole in argon atmosphere.

2. The thermal stability of poly(S-alt-MMA) is the same as other copolymers in helium, but worse than others in air. It is probably affected by the residual zinc ions — the complexing agent in copolymerization.

3. Polystyrene and polymethyl methacrylate have mutual stabilization effect when they are mixed together.

4. Hindered phenols stabilize S-MMA copolymers, but more stabilizer does not imply necessarily an increased stability.

5. S-MMA block copolymers have stronger mechanical properties than alternating and random copolymers.

6. For S-MMA copolymers, the alternating copolymer has the highest glass transition temperature, after is the block copolymer, and the random copolymer has the lowest glass temperature. The Tg of the random copolymer follow the empirical equation proposed to calculate a random copolymer's glass transition temperature.

7. S-MMA block copolymer has a little "compatibilizing" effect in PS-PMMA blend according to the dynamic mechanical test.

8. It is risky to regard the apparent activation energy of pyrolysis of a polymer as the criterion of its thermal stability.

Chapter VI

RECOMMENDATION

1. In order to know the mechanism of thermal degradation of poly(S-alt-MMA), we tried to plot residue molecular weight against thermal degradation time at constant temperature, but the residues were not soluble in THF, neither in toluene — the solvent used in selective precipitation while purifying poly(S-alt-MMA), we conclude that the residues are cross-linked. Maybe the thermal degradation in solution will avoid this problem.

2. Thermal stability of poly(S-alt-MMA) as a function of zinc concentration in the polymer is a interesting subject. It has been illustrated that zinc catalyzes the thermal degradation of poly(S-alt-MMA) in Section IV. 3. On the contrary, Kochneva and co-workers[86] found that zinc chloride reduced the rate of thermal and thermooxidative decomposition of polymethacrylic esters and increased the thermal decomposition rate of polyacrylic esters.

3. Thermal degradation of poly(S-alt-MMA) without zinc needs more study.

4. Since Rheovibron can not measure the entire glass transition of PS-PMMA blend, other instruments may be employed, such as torsion pendulum.

BIBLIOGRAPHY

1. Products catalogue of Richardson Co., Madison, Connecticut, USA.
2. A. Banderet, C. Tournut and G. Riess, J. Polym. Sci., C, 16, 914 (1967).
3. N. Hurduc, C. N. Cascaval, I. A. Schneider and G. Riess, Eur. Polym. J. 11, 429-35 (1975).
4. P. Bataille and F. Granger, Colloid Polym. Sci., 261, 914-12 (1983).
5. P. Bataille and F. Granger, J. Polym. Sci., Polym. Chem. ed., 23, 997-1007 (1985).
6. A. Dobry and F. Boyer-Kawenoki, J. Polym. Sci., 2, 90 (1947).
7. L. Bohn, Rubber Chem. Technol., 41, 495 (1968).
8. S. Krause, J. Macromol. Sci., Rev. Macromol. Chem., C7, 251 (1972).
9. J. H. Flynn, Aspects of Degradation and Stabilization of Polymers, edited by J. J. Jellinek, Elsevier, Amsterdam (1978).
10. E. S. Freeman and B. Carroll, J. Phys. Chem. 62, 394-7 (1958).
11. J. H. Flynn and L. A. Wall, J. Research Natl. Bur. Stad. Sect. A, 70(6), 487 (1966).

12. M. Letort, J. Chim. Phys. 34, 206 (1937).

13. C. D. Doyle, J. Appl. Polym. Sci., 6, 639-42 (1962).

14. J. H. Flynn and L. A. Wall, Polym. Letters, 4, 323-8 (1966).

15. C. D. Doyle, J. Appl. Polym. Sci., 5, 285-92 (1961).

16. R. Audebert and C. Aubineau, Eur. Polym. J., 6, 965-79 (1970).

17. W. L. Hawkins, Degradation and Stabilization of Polyolefins, edited by B. Sedlàcek et al, John Wiley & Sons (1976).

18. W. L. Hawkins, Degradation and Stabilization of Polymers, edited by G. Geuskens, John Wiley & Sons (1975).

19. E. A. Collins, J. Bares and F. W. Billmeyer, Experiments in Polymer Science, John Wiley & Sons (1973).

20. W. N. Findley, Trans. Plast. Inst., 30, 138 (1962).

21. D. G. O'Connor and W. N. Findley, Trans. SPE, 2, 273 (1962).

22. J. Marin and G. Cuff, Proc. ASTM, 49, 1158 (1949).

23. L. E. Nielsen, Mechanical Properties of Polymers and Composites, Marcel Dekker Inc., New York (1974).

24. J. D. Ferry, Viscoelastic Properties of Polymers, 2nd Ed., Wiley, New York (1970).

25. H. A. Waterman, Kolloid Zeit., 192 (1), 9 (1963).

26. W. P. Mason and H. J. McSkimin, Bell. Syst. Tech. J., 31 (1), 121 (1952).

27. P. Bataille, S. Boissé and H. P. Schreiber, Polym. Eng. Sci., 27 (9), 622-6 (1987).

28. P. Bataille, C. Jolicoeur and H. P. Schreiber, J. Vinyl Technol., 2 (4), 218-21 (1980).

29. J. W. Barlow and D. R. Paul, Polym. Eng. Sci., 24 (8), 525-34 (1984).

30. G. Riess, J. Periard, J. Kohier, Y. Jolivet and A. Banderet, Rev. Gen. Caout. Plast., 48 (4), 431-8 (1971).

31. G. E. Molau, J. Polym. Sci. A3, 1267 (1965).

32. G. E. Molau and W. M. Wittbrodt, Macromolecules, 1, 260 (1968).

33. T. Ouhadi, R. Fayt, R. Jérôme, Ph. Teyssié, J. Polym. Sci., Part B, 24, 973-81 (1986).

34. L. Del Giudice, R. E. Cohen, G. Attalla, F. Bertinotti, J. Appl. Polym. Sci., 30, 4305-18 (1985).

35. G. Riess, Makromol. Chem., Suppl. 13, 157-70 (1985).

36. J. Noolandi, K. M. Hong, Macromolecules, 17, 1531-37 (1984).

37. J. Noolandi, K. M. Hong, Macromolecules, 15, 482-92 (1982).

38. R. D. Deanin, S. B. Driscoll and J. T. Krowchun, Org. Coat. Plast. Chem. 40, 664-8 (1979).

39. D. J. Hourston and I. D. Hughes, Polymer, 19, 1181 (1978).

40. A. Beamish and D. J. Hourston, Polymer, 17, 577 (1976).

41. D. J. Hourston and I. D. Hughes, Polymer, 18, 1175 (1977).

42. D. J. Hourston and I. D. Hughes, Prep. Int. Rubber Conf. Brighton, 1, 1371 (1971).

43. Y. P. Singh, S. Das, S. Maiti and R. P. Singh, J. Pure Appl. Ultrason. 3, 1 (1981).

44. Y. P. Singh and R. P. Singh, Eur. Polym. J., 19 (6), 529-533 (1983).

45. Y. P. Singh and R. P. Singh, Eur. Polym. J. 19 (6), 535-541 (1983).

46. B. Schneier, J. Appl. Polym. Sci., 17. 3175 (1973).

47. C. Hugelin and A. Dondos, Makromol. Chem., 126, 206 (1969).

48. D. Feldmen and M. Rusu, Eur. Polym. J., 6, 627 (1970).

49. G. R. Williamson and B. Wright, J. Polym. Sci., Part A, 3, 3885 (1965).

50. C. Vasile, F. Sandru, I. A. Schneider and N. Asandei, Makromol. Chem., 110, 20 (1967).

51. C. Vasile, N. Asandei and I. A. Schneider, Rev. Roum. Chim., 11, 1247 (1966).

52. F. Lauzon, Summer Project, Dept. of Chem. Eng., Ecole Polytechnique of Montreal (1984).

53. D. E. Wilson and F. M. Hamaker, Ames Research Center NASA, private communication (1970).

54. D. A. Anderson and E. S. Freeman, J. Polym. Sci., 54, 253 (1961).

55. S. L. Madorsky, J. Polym. Sci., 9, 133 (1952).

56. D. W. Van Krevelen and P. J. Hoftyzer, Properties of Polymers, Elsevier Sci. Publ. Comp. (1976).

57. J. R. MacCallum, Macromol. Chem., 83, 137-47 (1965).

58. N. Grassie and H. W. Melville, Proc. Roy. Soc. (London) A199, 14-23 (1949).

59. N. Grassie and E. Farish, Europ. Polymer J., 3 (2), 305-15 (1967)

60. I. C. McNeill, Europ. Polymer J., 4 (1), 21-30 (1968).

61. J. C. Bevington, H. W. Melville and R. P. Taylor, J. Polym. Sci., 12, 449 (1954).

62. Patent, Jpn., Kokai Koho JP 57/135814 A2[82/135814], 5 pp (21 Aug 1982).

63. Sobunshi Ronbunshu, 33(2), 77-82.

64. Patent, Jpn., Kokai Tokkyo Koho JP 57/128744 A2[82/128744], 8pp (10 Aug 1982).

65. Patent, Jpn., Kokai Tokkyo Koho JP 60/32176 A2[85/32176], 7pp (19 Feb 1985).

66. Patent, Jpn., Kokai Tokkyo Koho JP 59/71351 A2[84/71351], 5 pp (23 Apr 1984).

67. Japanese patent, JP 46/10954 [71/10954], 4 pp (19 mars 1971).

68. Eur. Pat. Appl. EP 137519 A2, 100 pp, Designated States: DE, FR, GB, IT, NL. (17 Apr., 1985).

69. Yu. A. Shlyapnikov, V. B. Miller and E. S. Torsueva, Izvest Akad. Nauk SSSR, Otdel. Khim. Nauk, 1966 (1961).

70. R. F. Boyer, J. Polym. Sci., 9, 289-94 (1952).

71. H. W. McCormick, F. M. Brower and L. Kin, J. Polym. Sci., 39, 87-100 (1959).

72. T. G. Fox and P. J. Flory, J. Appl. Phys., 21, 581 (1950).

73. T. G. Fox and S. Loshaek, J. Polym. Sci., 15, 371-90 (1955).

74. R. B. Beevers and E. F. T. White, Trans. Faraday Soc., 56, 744-52 (1960).

75. T. G. Fox, Bull. Am. Phys. Soc., 1 (3), 123 (1956).

76. R. B. Beevers and E. F. T. White, Trans. Faraday Soc., 56, 1529-34 (1960).

77. S. Manabe, R. Murakami, M. Takayanagi and S. Uemura, Int. J. Polym. Mater., 1, 47 (1971).

78. L. J. Hughes and G. E. Britt, J. Appl. Polym. Sci., 5, 337 (1961).

79. S. D. Hong and C. M. Burns, J. Appl. Polym. Sci., 15, 1995 (1971).

80. V. P. Yartsev and S. B. Ratner, Dokl. Akad. Nauk SSSR, 290 (5), 1168-71 (1986).

81. D. J. Massa, Adv. Chem. Ser., 176, 433-42 (1979).

82. R. J. Peterson, R. D. Corneliussen and L. T. Rozelle, Polym. Prep. Am. Chem. Soc. Div. Polym. Chem., 10, 385 (1969).

83. O. Fuchs, Macromolek. Chem., 90, 293 (1966).

84. R. J. Kern, J. Polym. Sci., 21, 19 (1956).

85. D. R. Paul and S. Newman, Polymer Blends, Academic Press, New York (1978).

86. L. S. Kochneva, N. A. Kopylova, L. M. Terman and Yu. D. Semchikov, Eur. Polym. J., 15, 575-80 (1978).

87. P. Bataille and P. Grossetête, Chem. Eng. Comm., 51, 167-78 (1987).

APPENDIXES

Appendix I

Log p(Ea/RT) values for various Ea/RT[14,15]

Ea/RT	logp(Ea/RT)	Δlogp(Ea/RT)	Ea/RT	logp(Ea/RT)	Δlogp(Ea/RT)
7	4.830	-	34	17.853	0.459
8	5.369	0.593	35	18.312	0.459
9	5.898	0.528	36	18.770	0.458
10	6.416	0.518	37	19.228	0.458
11	6.928	0.511	38	19.684	0.456
12	7.433	0.505	39	20.141	0.456
13	7.933	0.500	40	20.596	0.456
14	8.427	0.494	41	21.052	0.455
15	8.918	0.491	42	21.507	0.455
16	9.406	0.488	43	21.961	0.454
17	9.890	0.484	44	22.415	0.454
18	10.372	0.482	45	22.868	0.453
19	10.851	0.479	46	23.321	0.453
20	11.327	0.477	47	23.774	0.453
21	11.803	0.475	48	24.226	0.452
22	12.276	0.473	49	24.678	0.452
23	12.747	0.471	50	25.129	0.451
24	13.217	0.470	51	25.580	0.451
25	13.686	0.469	52	26.031	0.450
26	14.153	0.467	53	26.482	0.450
27	14.619	0.466	54	26.932	0.450
28	15.084	0.465	55	27.382	0.450
29	15.547	0.463	56	27.831	0.449
30	16.010	0.463	57	28.281	0.449
31	16.472	0.462	58	28.730	0.449
32	16.933	0.461	59	29.179	0.448
33	17.394	0.461	60	29.628	0.448

Appendix II

COPOLYMERIZATION and CHARACTERIZATION of POLY(S-alt-MMA)

- Styrene and methyl methacrylate were washed three times with a 10% NaOH aqueous solution and then with distilled water in order to remove the inhibitors. The organic layers were dried over calcium chloride and distilled.

- 136.3g commercial anhydrous zinc chloride was dried at 150°C for two hours and put into an Erlenmeyer flask, 106ml methyl methacrylate is then added under agitation.

- The mixture was brought down to -15°C for 20 minutes in order to allow a complex between the monomer and the zinc chloride to form.

- The mixture was transferred to a 500ml reactor which is in the temperature controlled water bath at 40°C.

- 104ml styrene and 9ml distilled water were then added under agitation.

- After 18 hours of agitation, in order to separate

polymer, the reaction mixture was poured into a four liter container containing acidified methanol (1% HCl) in a ratio of 30 parts of methanol for one part of reaction mixture. The solution is then filtered through an Hirsch fritted glass funnel. The recovered polymer was purified by selective precipitation using toluene as the solvent and ether as the non-solvent[52].

Atomic absorption spectroscopy shows that the obtained polymer contains 0.2% zinc by weight.

The NMR spectrum of the poly(S-alt-MMA) is shown in Fig. 49. Observations on this spectrum are:

a) There is no successive styrene units as there is no peak corresponding to the "ortho" proton in the phenyl group in the NMR spectrum.

b) The non-existence of a methoxy triad at 3.62ppm indicates that there is a methyl methacrylate sequence but no polymethyl methacrylate.

c) The existence of 3 peaks attributed to the methyl protons at 2.3ppm, 3.0ppm and 3.4ppm corresponds to the three cosyndiotactic, coheterotactic and coisotactic indicates that the copolymer is atactic[87].

Thus the polymer is an alternating copolymer.

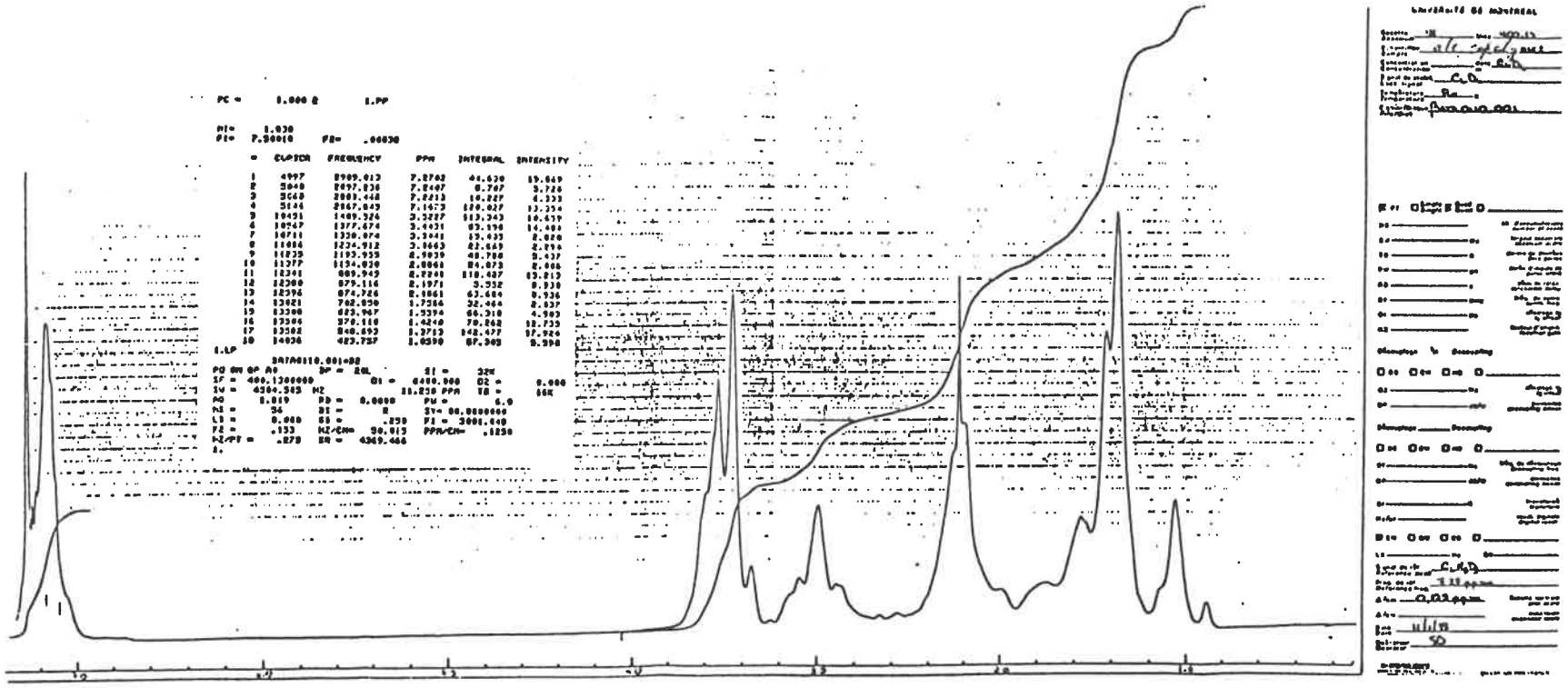

Fig. 49 NMR spectrum of poly(S-alt-MMA).

Appendix III

Calculation Procedure in Isothermal Method

$$\ln(-dw_t/dt) = \ln(A) - Ea/RT + n*\ln(w_t) \qquad (9)$$

The experiment was carried out under isothermal conditions, the residue weight at time t (w_t) and the degradation rate at the same time ($-dw_t/dt$) were read from the TG curve. Then, a graph of $\ln(-dw_t/dt)$ versus $\ln(w_t)$ was made. For every isothermal test, a straight line was determined by least-square method with an IBM micro-computer, both slope and intercept were given automatically, see Fig. 50. Here, the degradation of poly(S-alt-MMA) in air atmosphere was taken as an example. According to Equ. 9, the slope gives the reaction order, and the intercepts serve to calculate the activation energy. In the case of Fig. 50,

$$\text{intercept} = \ln(A) - Ea/RT \qquad \text{from Equ. 9}$$

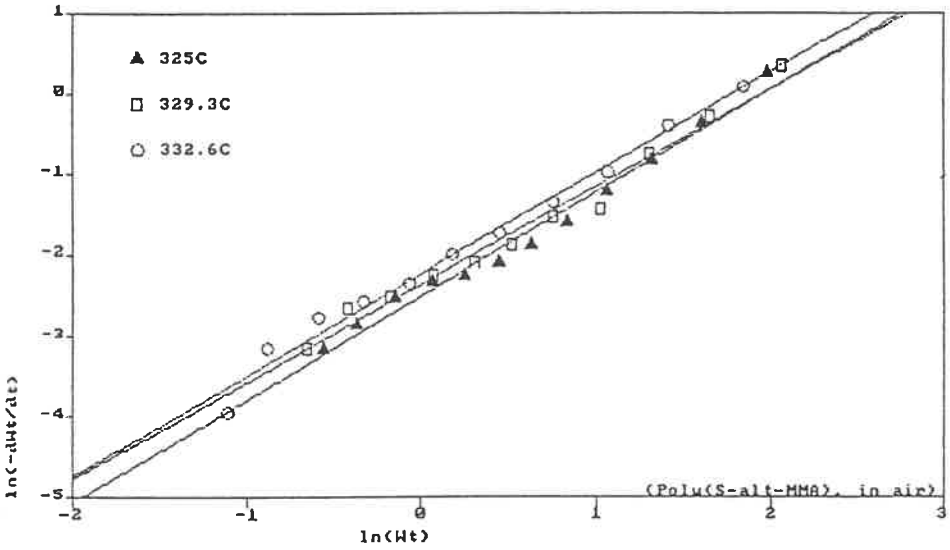

THE REGRESSION POLYNOMIAL OF LINE 1 -

(-2.504E+00) + (1.278E+00)*X
THE VARIANCE - 1.800E-02

THE REGRESSION POLYNOMIAL OF LINE 2 -

(-2.360E+00) + (1.206E+00)*X
THE VARIANCE - 2.236E-02

THE REGRESSION POLYNOMIAL OF LINE 3 -

(-2.233E+00) + (1.248E+00)*X
THE VARIANCE - 1.865E-02

Fig. 50 Linear regression in isothermal method.

$$-2.504 = \ln(A) - Ea/(325+273)R \qquad \text{line 1} \quad (56)$$

$$-2.360 = \ln(A) - Ea/(329.3+273)R \qquad \text{line 2} \quad (57)$$

$$-2.233 = \ln(A) - Ea/(332.6+273)R \qquad \text{line 3} \quad (58)$$

$$e^{-2.504} = A*e^{-Ea/598R} \qquad \text{line 1} \quad (56)$$

$$e^{-2.360} = A*e^{-Ea/602.3R} \qquad \text{line 2} \quad (57)$$

$$e^{-2.233} = A*e^{-Ea/605.6R} \qquad \text{line 3} \quad (58)$$

(57)/(58), Ea = 23.97 (kcal/mole)

(57)/(59), Ea = 25.66 (kcal/mole)

(58)/(59), Ea = 27.89 (kcal/mole)

$$\bar{E}a = 25.84 \pm 1.60 \text{ (kcal/mole)}$$

$$= 108.1 \pm 6.7 \text{ (kJ/mole)} \qquad (59)$$

Reaction order = slope = 1.2 (60)

The calculations for other degradations are the same, except for PS degrades in air atmosphere and poly(S-alt-MMA) in helium atmosphere, only two isothermal tests were done, so that the standard deviation of Ea in these two cases could not be calculated, see Table 2.

Appendix IV

Calculation Procedure in multi-Experimental Comparison Method

$$\log F(\alpha) = \log(AEa/R) - \log \beta + \log p(Ea/RT) \quad (18)$$

$$\log p(Ea/RT) \approx -2.315 - 0.457Ea/RT \quad (19)$$

log p(Ea/RT) values for various Ea/RT is listed in Appendix I. log p(Ea/RT) is not an absolute linear function of Ea/RT, see Fig. 51. The Δlog p(Ea/RT) column in Appendix I displays the slopes at varying Ea/RT values. Substituting Equ. 19 into Equ. 18, one obtains

$$\log F(\alpha) \approx \log(AEa/R) - \log \beta - 2.315 - 0.457Ea/RT$$

$$\approx \text{constant} - \log \beta - 0.457Ea/RT \quad (20)$$

Thus, under fixed conversion α, Equ. 20 can be written as

$$\log \beta \approx \text{constant} - \log F(\alpha) - 0.457Ea/RT$$

$$\approx \text{constant} - 0.457 \frac{Ea}{R} \frac{1}{T} \quad (61)$$

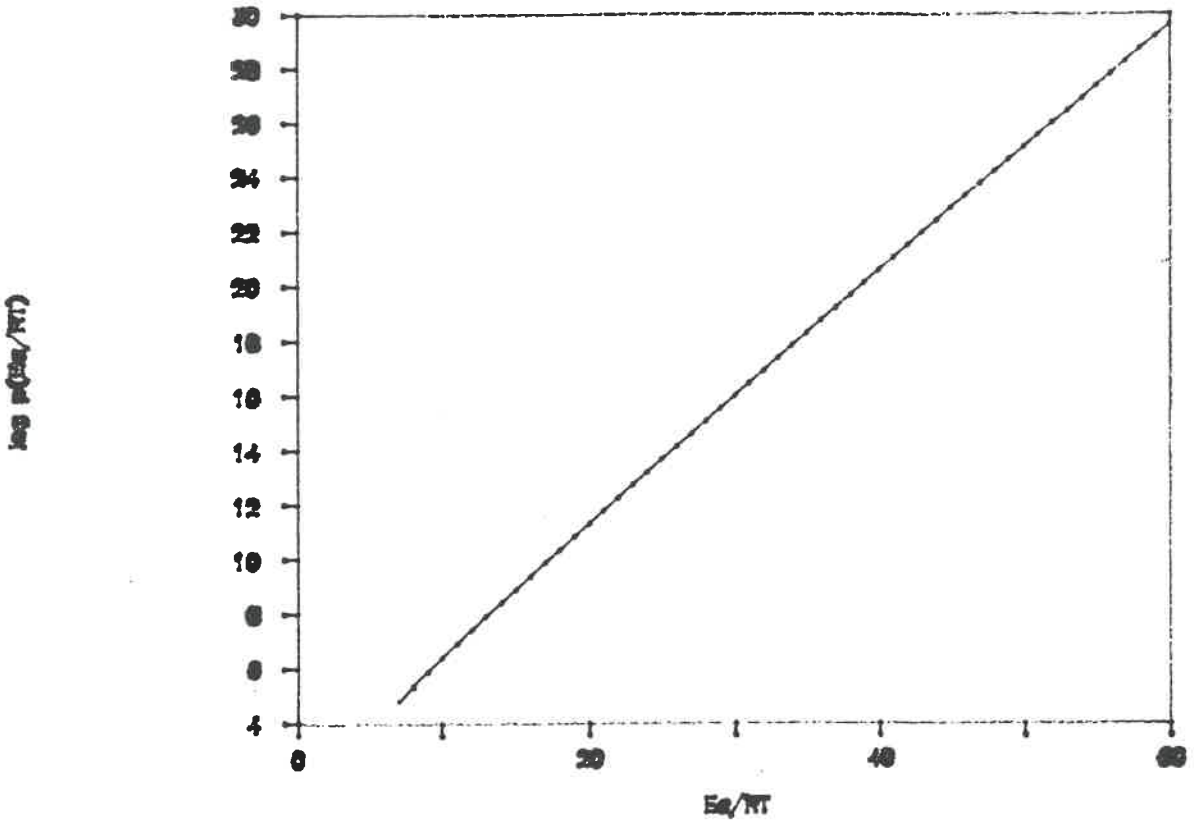

Fig. 51 log p(Ea/RT) versus Ea/RT graph.

The experiment was performed under different heating rate β. For conversions from 10% to 90% by step of 10%, a graph of log β versus 1/T was done, see Fig. 52, the example is the thermal degradation of poly(S-alt-MMA) in argon atmosphere. For every conversion α, linear regression of least-square method was done with an IBM microcomputer. Fig. 52 shows that while the conversion α = 0.1, the plot is not parallel to those at other conversions. This denotes that the activation energy at 0.1 conversion is different from what at other conversions, therefore, the Ea was calculated from conversion 0.2 to 0.9.

First, the values of slopes of every plot were listed in Table 11 after the column of conversion α. Next, the approximate activation energies ($Ea_{approx.}$) were calculated in the third column according to Equ. 61:

$$\text{slope} \approx -0.457Ea/R \qquad (62)$$

Third, the corresponding temperatures were read from TG curves and listed in column 4. After this, the approximate values of Ea/RT were obtained from the third and fourth columns, see column 5. Fifth, the approximate Ea/RT values in column 5 were used to reevaluated the constant, -0.457, in Equ. 61 according to Appendix I, the results are written in column 6. At last, the corrected activation

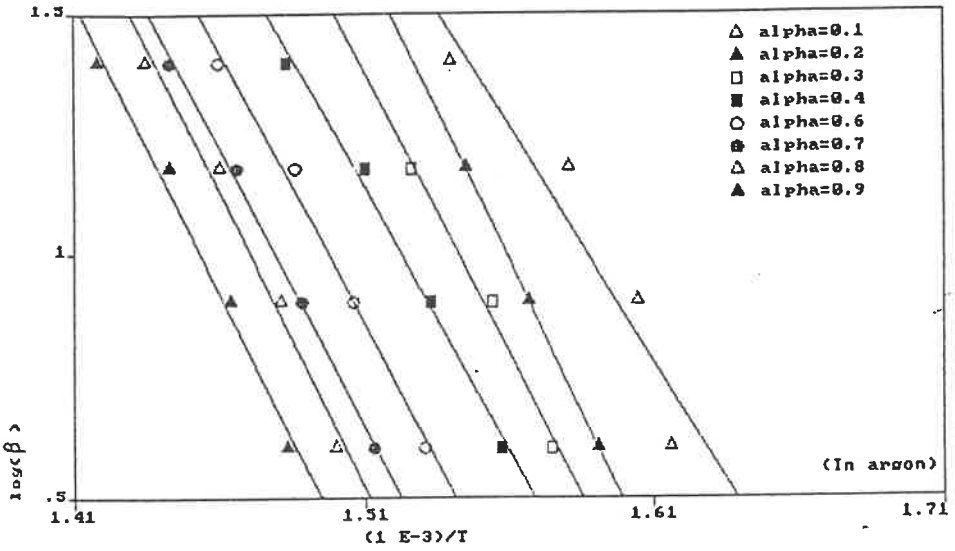

THE REGRESSION POLYNOMIAL OF LINE 1 -

(1.638E+01) + (-9.686E+00)*X
THE VARIANCE - 9.190E-03

THE REGRESSION POLYNOMIAL OF LINE 2 -

(2.046E+01) + (-1.248E+01)*X
THE VARIANCE - 5.167E-07

THE REGRESSION POLYNOMIAL OF LINE 3 -

(1.889E+01) + (-1.160E+01)*X
THE VARIANCE - 6.677E-04

THE REGRESSION POLYNOMIAL OF LINE 4 -

(1.749E+01) + (-1.083E+01)*X
THE VARIANCE - 8.520E-04

THE REGRESSION POLYNOMIAL OF LINE 5 -

(1.793E+01) + (-1.131E+01)*X
THE VARIANCE - 8.694E-04

THE REGRESSION POLYNOMIAL OF LINE 6 -

(1.797E+01) + (-1.147E+01)*X
THE VARIANCE - 2.557E-04

THE REGRESSION POLYNOMIAL OF LINE 7 -

(1.897E+01) + (-1.222E+01)*X
THE VARIANCE - 1.484E-03

THE REGRESSION POLYNOMIAL OF LINE 8 -

(1.875E+01) + (-1.221E+01)*X
THE VARIANCE - 1.484E-03

Fig. 52 Linear regression in Multi-Experimental Comparison Method.

energies $Ea_{corrected}$ were figured by employing Equ. 62 and the reevaluated constants in column 6, see column 7. From column 7, the average activation energy and its standard deviation was determined.

Repeating the steps 4,5,6 in the previous procedure, the Ea's obtained in column 10 is more accurate than those in column 7, but the improvement is very small: 0.1 kJ/mole —— 0.05% amelioration for the activation energy, and 0.1 kJ/mole —— 1.0% amelioration for the standard deviation. This is in agree with Audebert et al.'s work[16], they has found that a single iteration is sufficient.

The first 7 columns in Table 11 is exactly the second part of Table 3.

Table 11 Calculation procedure of Ea of poly(S-alt-MMA) degradation in argon atmosphere by multi-experimental comparison method

Conversion α	slope 10^{-3}	$Ea_{approx.}$ (kcal/mole)	T (K)	First iteration Ea/RT (approx.)	Reevaluated constant	$Ea_{corrected}$ (kcal/mole)
Poly (S-alt-MMA) degrades in argon						
0.2	-12.48	54.26	628.4	43.45	0.4540	54.62
0.3	-11.60	50.44	634.8	39.33	0.4560	50.55
0.4	-10.83	47.09	642.2	36.90	0.4580	46.98
0.6	-11.31	49.17	653.1	37.89	0.4562	49.26
0.7	-11.47	49.87	661.2	37.96	0.4561	49.97
0.8	-12.22	53.13	665.6	40.17	0.4558	53.27
0.9	-12.21	53.09	674.1	39.63	0.4560	53.20
Ea (in argon, conversion 0.2-0.9): 51.12 ± 2.49 kcal/mole = 213.9 ± 10.4 kJ/mole						

Second iteration Ea/RT (approx.)	Reevaluated constant	$Ea_{corrected}$ (kcal/mole)
43.74	0.454	54.62
40.08	0.456	50.55
36.82	0.458	46.98
37.99	0.456	49.28
38.03	0.456	49.98
40.28	0.4557	53.28
36.47	0.458	52.97
Ea = 51.09 ± 2.46 kcal/mole = 213.8 ± 10.3 kJ/mole		

Appendix V

IRGANOX 1010

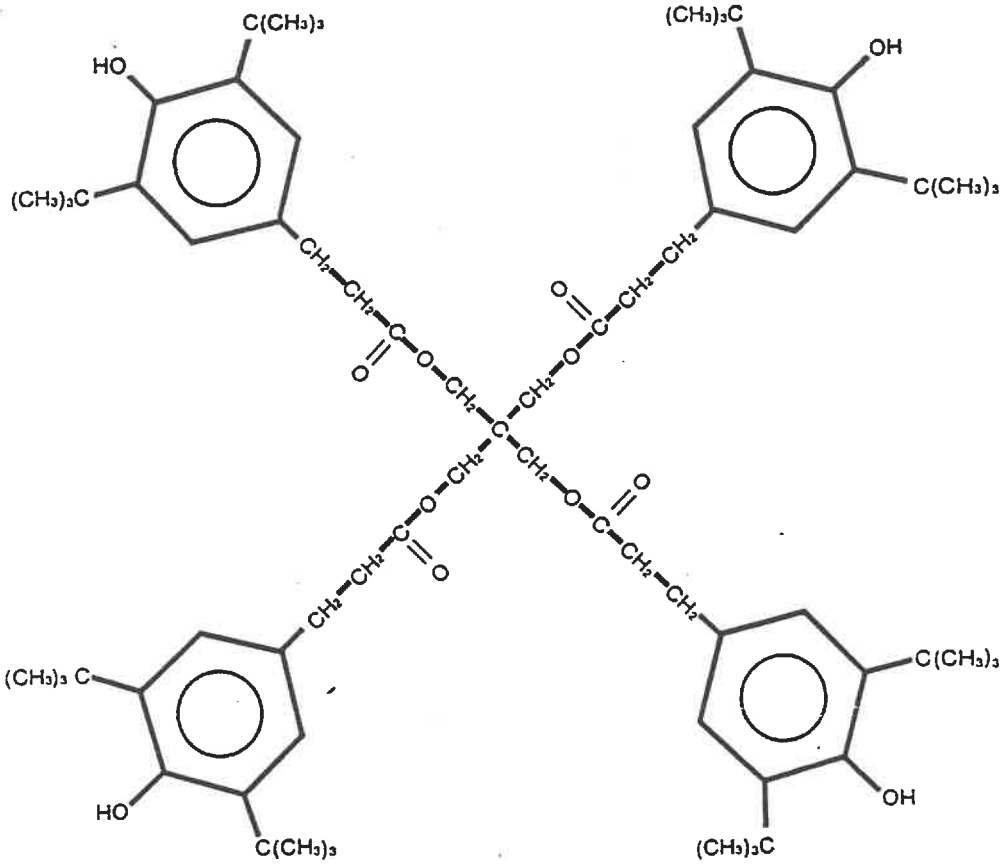

Irganox MD-1024